

1 REPLY TO REVIEWER #1'S REMARKS

2  
3 on the manuscript acp-2014-540: "Meridional distribution of aerosol optical thickness over  
4 the tropical Atlantic Ocean"

5 by P. Kishcha, A.M. da Silva, B. Starobinets, C.N. Long, O. Kalashnikova, and P. Alpert.  
6

7 We would like to thank Reviewer #1 for his valuable remarks. These remarks have been taken  
8 into account in the revised manuscript, as listed below.  
9

10 ***"Anonymous Referee #1***

11 *Received and published: 17 September 2014*  
12

13 *This paper analyzes satellite products and assimilated data sets over the tropical Atlantic to explore*  
14 *the meridional distribution of aerosol, cloud and rainfall products. The paper is well-written. Previous*  
15 *literature is well-referenced. By using MERRAero data for their aerosol, which is satellite-assisted*  
16 *model results, the authors can distinguish between different aerosol types, including dust and OC/BC*  
17 *that is associated with biomass burning smoke in their area of study. This is a nice capability not*  
18 *directly available from satellite products. The MERRAero total aerosol optical depth is compared with*  
19 *MISR products and looks really, really good. The cloud fraction data are taken directly from MODIS*  
20 *aerosol products, as are the rainfall products taken directly from TRMM.*  
21

22 *The authors use their data set to identify both temporal and spatial associations between total aerosol,*  
23 *aerosol types, cloud fraction and precipitation. They show that some of the asymmetry in cloud*  
24 *fraction between northern and southern hemispheres is linked to the migration of the ITCZ and its*  
25 *hemispherical asymmetry. However, they note a spatial association between the location of the dust*  
26 *and maximums in the cloud fraction. The authors imply, but do not state in their conclusions, that*  
27 *increasing cloud fraction is due, in part, to increased aerosol loading.*  
28

29 *From my perspective, these results are interesting without being important. Without a conclusion that*  
30 *discusses the possible reason(s) for these observed associations, the paper adds little value for the*  
31 *community.*  
32

33 Our main point is that, over the tropical Atlantic, not only is Saharan dust responsible for the  
34 hemispheric aerosol asymmetry, but it also contributes to significant cloud fraction along the  
35 Saharan Air Layer. This significant cloud fraction in the area of SAL together with clouds  
36 over the Atlantic Inter-tropical Convergence Zone contributes to hemispheric asymmetry in  
37 cloud cover over the tropical Atlantic. This could lead to the hemispheric imbalance in strong  
38 solar radiation reaching the sea surface over the tropical Atlantic. The phenomenon of  
39 significant CF along SAL is important to the community and has not been reported so far, to  
40 our knowledge.  
41

42 In accordance with the Reviewer's remarks, in the revised version, new Sections 4.4.2 and  
43 4.5.3 have been added (Pages 11 – 13), where we discuss physical mechanisms for the  
44 formation of significant CF along SAL. Both the Abstract and the title have been updated  
45 (Pages 1 - 2).  
46

47 *"Discussing possible reasons for these associations is not easy. My first thought is that the MODIS*  
48 *Cloud Fraction is contaminated by heavy aerosol loading and that is why the associations are so*  
49 *strong. There are several different cloud fraction products available from MODIS. I believe the*  
50 *authors are using the cloud fraction that is derived from the standard cloud mask (MOD35). The*  
51 *purpose of this mask is to identify clouds, but to err on the side of preventing "leakage". It may very*  
52 *well call heavy aerosol "cloudy."*

1  
2 We appreciate this Reviewer’s comment which led us to clarify this point in the revised  
3 version (the new Section 4.5.3, Page 13).

4 Indeed, Collection 5 of MODIS-Terra monthly daytime cloud fraction data used are derived  
5 from the standard cloud mask product based on the cloud mask algorithm MOD35 (Ackerman  
6 et al., 1998, Frey et al., 2008). In heavy dust loading situations, such as dust storms over  
7 deserts, MOD35 may flag the aerosol-laden atmosphere as cloudy (Ackerman et al., 1998).

8 During dust storms over deserts, observed AOT values range from 2 to 5 (e.g. Alam et al.,  
9 2014). However, over the tropical North Atlantic, strong AOT exceeding even 1 is a very rare  
10 phenomenon. To demonstrate that AOT exceeding 1 is a rare phenomenon over the tropical  
11 North Atlantic, Fig. 12a represents a histogram of AOT observed over the tropical North  
12 Atlantic in July, 2010, based on MODIS Level 3 AOT daily data. July 2010 was chosen  
13 because AOT, averaged over the tropical North Atlantic, was maximal compared to AOT in  
14 other July months, during the 10-year study period. One can see that AOT hardly exceed 1. A  
15 similar situation can be seen over the latitudes with SAL presence (12°N – 24°N) (Fig. 12b).  
16 Therefore, the effect of MODIS cloud fraction contamination by heavy dust loading cannot  
17 essentially contribute to averaging CF over the tropical North Atlantic. Consequently, given  
18 the large amount of available MODIS CF daily data over the 10-year study period, cloud  
19 fraction contamination does not account for the obtained hemispheric CF asymmetry.

20  
21 *“There are other possible reasons for the observed associations, including some that are physical*  
22 *mechanisms. However, it would surprise me if cloud fraction is increasing through the Albrecht*  
23 *(1989) mechanism. Here in this study the authors find the strongest relationship between aerosol and*  
24 *cloud fraction when the aerosol is very thick. We know to expect the strongest relationships when*  
25 *clouds are starved for CCN, when aerosol goes from pristine to moderately loaded (Koren et al.,*  
26 *2008, 2014). A physical possibility may be a pathway that involves ice nuclei and ice processes. All*  
27 *we see here is cloud fraction, so we don’t know if the association between aerosol and clouds affects*  
28 *water clouds, ice clouds or both. “*

29  
30 We agree with the Reviewer that the Albrecht (1989) mechanism is not suitable for the SAL  
31 area with heavy dust loading.

32 As discussed in the revised version (Section 4.5.3, Pages 11 - 13), we consider that the most  
33 likely physical mechanism for the formation of significant cloud cover along SAL is as  
34 follows:

35 The observed temperature inversion over zones 1 - 4 prevents deep cloud formation; this  
36 explains limited precipitation in these zones. On the other hand, meteorological conditions  
37 below the temperature inversion at the SAL base include significant atmospheric humidity  
38 and the presence of large amounts of settling dust particles together with marine aerosols.

39 As known, aerosol species often combine to form mixed particles, with properties different  
40 from those of their components (Andreae et al., 2009). Mineral dust particles are known to be  
41 not very efficient cloud condensation nuclei (CCN), unless they are coated with soluble  
42 materials (Andreae et al., 2009). Using airplane measurements, Levin et al. (2005) showed  
43 that dust transport over the sea could lead to sea-salt coating on dust particles. Coating settling  
44 dust particles with sea-salt could modify them into efficient CCN. Being below the  
45 temperature inversion and acting as efficient CCN, Saharan dust particles coated with soluble  
46 material contribute to the formation of shallow stratocumulus clouds. This physical  
47 mechanism, based on the indirect effect of Saharan dust on stratocumulus clouds below the  
48 temperature inversion, could explain the observed significant cloud cover (CF up to 0.8 – 0.9)  
49 along the Saharan Air Layer. The significant cloud fraction along SAL contributes to

1 hemispheric CF asymmetry over the tropical Atlantic. This could lead to hemispheric  
2 imbalance in strong solar radiation reaching the sea surface in the tropical Atlantic Ocean.  
3 To examine the properties of clouds in the area of SAL, we analyzed available data on the  
4 effective radius of cloud droplets. Fig. 11 represents histograms of the effective radius (Reff)  
5 of cloud droplets for liquid water clouds in the specified zones 1 – 4 along SAL, based on  
6 MODIS L3 gridded monthly data (1° x 1°) during the 10-year study period in July. The data  
7 were supplied by the Giovanni data base. It is obvious that the cloud droplet effective radius  
8 increases from zone 1 to zone 4 (Fig. 11). One can see a systematic shift in the whole  
9 histogram to higher values of Reff from zone 1 to zone 4. This can be explained by the  
10 decrease in CCN numbers associated with the decreasing numbers of settling Saharan dust  
11 particles with distance from the Sahara, in accordance with the decrease in dust AOT shown  
12 in Fig. 9a.

13 Thus, the cloud droplet effective radius in zone 4 was larger than in zones 1 - 3. This could  
14 lead to some increase in precipitation in zone 4. Indeed, as shown in Fig. 9b, TRMM  
15 accumulated rainfall in zone 4 was more intensive than over zones 1 - 3. This supports the  
16 above-mentioned physical mechanism of cloud formation below the temperature inversion at  
17 the SAL base.

18  
19 *“When the aerosol is very thick it should create a temperature signal in the vertical temperature*  
20 *profiles because both dust and OC/BC are absorbing aerosols that absorb sunlight and heat the*  
21 *column (Alpert et al., 1998; Ackerman et al., 2000; Koren et al. 2008). The more aerosol, the greater*  
22 *the amount of heating. Most studies associate this heating with a suppression of cloudiness, so that*  
23 *there should be a negative correlation between aerosol loading and cloud fraction. I know of one*  
24 *paper by Johnson et al. (2004), that finds a physical mechanism that can explain increased cloudiness,*  
25 *due to the heating, in this region. There may be others.”*

26  
27 Saharan dust particles can influence the vertical temperature profile in the atmosphere directly  
28 by absorbing solar radiation. Aerosol absorption by Saharan dust may decrease cloud cover  
29 by heating the air and reducing relative humidity (the semi-direct aerosol effect) (Johnson et  
30 al., 2004, Kaufman et al., 2005b). So that there should be a negative correlation between dust  
31 loading and cloud fraction along SAL. However, this is not the case: both dust AOT and CF  
32 decrease with the distance from the Sahara (Figs. 8b and 9b).

33  
34 *Anyway there are several possible reasons why we see these associations, some because of artifacts or*  
35 *co-varying meteorology, and some perhaps because aerosols are influencing the clouds through*  
36 *microphysics or by changing the environment in which the clouds evolve. Simply discussing all the*  
37 *possibilities, as I have done here, still only lifts the paper to the mediocre level. Some attempt should*  
38 *be made to PROVE which possibility is the most likely.”*

39 *There is nothing WRONG with the analysis presented in this paper, but I question whether simply*  
40 *presenting the results of the analysis with no conclusion is worth publication. I do not recommend*  
41 *publishing this paper in this form.*

42  
43 We do not agree that significant CF along SAL is an artifact. As mentioned in our reply to the  
44 previous Reviewer’s comment on this topic, the effect of MODIS cloud contamination by  
45 heavy dust loading does not account for meridional CF asymmetry over the tropical Atlantic  
46 (see a new section 4.5.3, Page 13). Therefore, the hemispheric 20% CF asymmetry found in  
47 the summer months is a real phenomenon. The hemispheric CF asymmetry could lead to the  
48 hemispheric imbalance in surface solar radiation over the tropical Atlantic. We feel that  
49 reporting important findings is worthy of publication. In the revised version (a new section

1 4.5.2, Pages 11 - 13) we discuss the most likely physical mechanism for the formation of  
2 significant cloud cover along SAL in July.

3  
4 *Minor comments:*

5 *My comments are linked to the web-based (non printer friendly) version of the paper.*

6  
7 *p. 23312 lines 17-23. Why does the meridional distribution of aerosol and cloud fraction matter?*  
8 *Nowhere in the introduction do the authors explain their motivation for doing this study.*

9  
10 Hemispheric asymmetry in cloud fraction (CF) and aerosols could lead to hemispheric  
11 imbalance in surface solar radiation. Consequently, analyzing hemispheric asymmetry in CF  
12 and aerosols is essential for understanding climate formation and its changes. Previous studies  
13 showed that, over the global ocean, there is hemispheric asymmetry in aerosols and no  
14 noticeable asymmetry in cloud fraction (CF). This contributes to the hemispheric balance in  
15 solar radiation reaching the sea surface. We chose the tropical Atlantic because it is  
16 characterized by significant amounts of Saharan dust dominating other aerosol species over  
17 the North Atlantic. We wished to find out if the meridional CF distribution remains  
18 symmetrical in the presence of such strong hemispheric aerosol asymmetry. This explains our  
19 motivation for doing the current study (Page 3, lines 22 – 25).

20  
21 *P23313 line22 and throughout the manuscript. The authors use ten yr to denote ten-year or 10-year*  
22 *without explaining what yr stands for. The journal style book may disagree with me, but I feel that ten-*  
23 *year or 10-year is better.*

24  
25 This was determined by the production editor, in accordance with the ACP journal style. In  
26 our original version, we used the same expressions as suggested by the Reviewer.

27  
28 *P23314 lines 23-25. Reference Frey et al. (2008) or Ackerman et al. (1998) so that we*  
29 *know that this is derived from MOD35.*

30  
31 Done. (Page 5, line 21)

32  
33 *P23316 line 15. Here we have 10yr, which I really prefer to be 10-year.*

34  
35 See our reply to the previous similar remark.

36  
37 *P23316 line 16. “much more” should be “many more”*

38  
39 Done. (Page 7, line 2)

40  
41 *P23321 lines 15-16. Do the authors know for sure that it is gravitational settling? Could it not be wet*  
42 *deposition? All that implied aerosol-cloud interaction and I would expect that a lot of aerosol is*  
43 *leaving the atmosphere because of washing out in the rain.*

44  
45 Indeed, rainfall always removes aerosols. However, as shown in Fig. 9, a strong decrease in  
46 dust AOT from zone 1 to zone 3 was not accompanied by any changes in TRMM  
47 accumulated rainfall. Therefore, the washing out of aerosols by rainfall does not account for  
48 the aerosol spatial decrease with distance from the Sahara. It proves that gravitational settling  
49 of Saharan dust particles accounts for this dust spatial decrease with distance from the Sahara.  
50 (Page 11, lines 9 – 14).

1  
2 *“Figures 9 and 10, and associated discussion in the text. You lose the inversion as you travel from*  
3 *zone 1 to zone 6. Meanwhile the convection intensifies. The authors see this as cause and effect, which*  
4 *I’m willing to accept. However, the cloudiness decreases. More convection, but less cloud cover.*  
5 *Earlier in the paper the authors noted that in the north-south direction the peak in cloudiness*  
6 *corresponded to the peak in convection, but here in the east-west direction the opposite is true. This*  
7 *only points out that the full story is still hidden.*

8  
9 The Reviewer should note that, in the current study, we focus on the relationship between  
10 temperature inversion and convection over the area of SAL, and not over the Atlantic Inter-  
11 tropical convergence zone.

12 Let us start with the east-west direction. We lose inversion over zone 5 and 6. Significant  
13 precipitation in zones 5 and 6 (up to 110 mm month<sup>-1</sup>) indicates the presence of developed  
14 clouds which are characterized by increased cloud thickness. These clouds over zones 5 and 6  
15 differ from shallow stratocumulus clouds created under the temperature inversion in zones 1 –  
16 4. The thick developed clouds over zones 5 and 6 may create CF lower than that created by  
17 the shallow stratocumulus clouds over zones 1 – 4.

18 In the north-south direction, the first peak in CF corresponds to the peak in convection in the  
19 Atlantic Inter-tropical convergence zone centered at approximately 8°N in July (Fig. 7).  
20 However, the second peak in CF is seen over the SAL zone centered at approximately 18°N  
21 (Fig. 7). The first CF peak (centered at 8°N) is created over the area with maximal convection,  
22 while the second CF peak (centered at 18°N) is created over the area with minimal convection  
23 because of the presence of temperature inversion. Contrary to the Reviewer’s opinion, we  
24 found that, in the north – south direction over the SAL area, there is no direct relationship  
25 between CF and convection.

26  
27 *“How are cloud types and morphology changing? How do these changes associate with the different*  
28 *types of aerosol?”*

29  
30 There are different cloud types over zones 1 – 4 on the one hand, and over zones 5 – 6 on the  
31 other hand. Over zones 1 – 4, we consider the presence of shallow stratocumulus clouds  
32 below the temperature inversion at the SAL base. These shallow stratocumulus clouds are  
33 characterized by limited precipitation. Over zones 5 – 6, we consider the presence of  
34 developed clouds capable of producing strong precipitation up to 110 mm month<sup>-1</sup>.

35  
36 *“Is there a possibility that the aerosol absorption is contributing to the strength of the inversion? Lots*  
37 *and lots of questions that should be answered or at least partly answered.”*

38  
39 The answer is in the affirmative. As mentioned in the manuscript, Saharan dust travels across  
40 the Atlantic Ocean within the hot and dry Saharan Air Layer with temperature inversion at the  
41 SAL base. In addition, the direct radiation effect of dust aerosols (i.e. absorption of solar  
42 radiation) could contribute to the strength of inversion. As seen in Fig. 10, the temperature  
43 inversion over zone 1 (in the presence of a large amount of dust) is stronger than over zone 4  
44 where the amount of dust is lower than over zone 1.

45  
46 References:

47 Ackerman, S.A., Strabala, K.I., Menzel, W.P., Frey, R.A., Moeller, C.C., and Gumley, L.E.:  
48 Discriminating clear sky from clouds with MODIS, *J. Geophys. Res.*, 103(D24), 32141–  
49 32157, doi:10.1029/1998JD200032, 1998.

50 Ackerman, A.S., O.B. Toon, D.E. Stevens, A.J. Heymsfield, V. Ramanathan, and E.J.

1 Welton: Reduction of tropical cloudiness by soot. *Science*, 288, 1042-1047,  
2 doi:10.1126/science.288.5468.1042, 2000.

3 Albrecht, B.A.: *Science*, 245, 1227-1230, DOI: 10.1126/science.245.4923.1227, 1989.

4 Alam, K., Trautmann, T., Blaschke, T., Subhand, F.: Changes in aerosol optical properties  
5 due to dust storms in the Middle East and Southwest Asia *Remote Sensing of Environment*,  
6 143, 216–227, 2014.

7 Alpert, P., Kaufman, Y.J., Shay-El, Y., Tanre, D., da Silva, A., Schubert, S., and Joseph, J.H.:  
8 Quantification of dust-forced heating of the lower troposphere. *Nature* 395, 367-370, 1998.

9 Andreae, M.O., Hegg, D.A., and Baltensperger, U.: Sources and nature of atmospheric  
10 aerosols. In *Aerosol pollution impact on precipitation*. Eds.: Z. Levin and W. Cotton.  
11 Springer, Chapter 3, 45 – 90, 2009.

12 Frey, R.A., Ackerman, S.A., Liu, Y., Strabala, K.I., Zhang, H., Key, J.R., Wang, X.: Cloud  
13 detection with MODIS. Part I: Improvements in the MODIS cloud mask for Collection 5. *J.*  
14 *Atmos. Ocean. Tech.*, 25, 1057 – 1072, 2008.

15 Johnson, B.T., K.P. Shine and P.M. Forster: The semi-direct aerosol effect: Impact of  
16 absorbing aerosols on marine stratocumulus. *Quart. J. Roy. Meteorol. Soc.*, 130,  
17 1407-1422 , 2004.

18 Koren, I., G. Dagan, and O. Altaratz: From aerosol-limited to invigoration of warm  
19 convective clouds, *Science*, 344(6188), 1143-1146., 2014

20 Koren, Ilan, J. Vanderlei Martins, Lorraine A. Remer, Hila Afargan, 2008: Smoke  
21 Invigoration Versus Inhibition of Clouds over the Amazon, *Science*, 321. 946 – 949  
22 DOI/10.1126:science.1159185 2008

23 Levin, Z., Teller, A., Ganor, E., and Yin, Y.: On the interactions of mineral dust, sea-salt  
24 particles, and clouds: A measurement and modeling study from the Mediterranean Israeli  
25 Dust Experiment campaign, *J. Geophys. Res.*, 110, D20202, doi:10.1029/2005JD005810,  
26 2005.

27 Interactive comment on *Atmos. Chem. Phys. Discuss.*, 14, 23309, 2014.

28

29

30



# Hemispheric asymmetry in aerosol optical thickness and cloud fraction over the tropical Atlantic Ocean

P. Kishcha<sup>1</sup>, A.M. da Silva<sup>2</sup>, B. Starobinets<sup>1</sup>, C.N. Long<sup>3</sup>, O. Kalashnikova<sup>4</sup>, and P. Alpert<sup>1</sup>

[1]{Department of Geosciences, Tel-Aviv University, Tel-Aviv, Israel}

[2]{Global Modeling and Assimilation Office, NASA/GSFC, Greenbelt, Maryland USA}

[3]{Pacific Northwest National Laboratory, Richland, Washington, USA}

[4]{Jet Propulsion Laboratory, California Institute of Technology, Pasadena, CA 91109, USA }

Correspondence to: P. Kishcha (pavelk@post.tau.ac.il)

## Abstract

Previous studies showed that, over the global ocean, there is no noticeable hemispheric asymmetry in cloud fraction (CF). **This contributes to the balance in solar radiation reaching the sea surface in the Northern and Southern hemispheres.** In the current study, we focus on the tropical Atlantic (30°N – 30°S) which is characterized by significant amounts of Saharan dust dominating other aerosol species over the North Atlantic. **Our main point is that, over the tropical Atlantic, not only is Saharan dust responsible for the pronounced hemispheric aerosol asymmetry, but it also contributes to significant cloud cover along the Saharan Air Layer.** **This could lead to the hemispheric imbalance in strong solar radiation reaching the sea surface in the tropical Atlantic.** During the 10-year study period (July 2002 – June 2012), NASA Aerosol Reanalysis (aka MERRAero) showed that, when the hemispheric asymmetry in dust aerosol optical thickness (AOT) was the most pronounced (particularly in July), dust AOT averaged separately over the tropical North Atlantic was one order of magnitude higher than that averaged over the tropical South Atlantic. In the presence of such strong hemispheric asymmetry in dust AOT in July, CF averaged separately over the tropical North Atlantic



1 exceeded that over the tropical South Atlantic by 20%. In July, along the Saharan Air Layer,  
2 Moderate Resolution Imaging Spectroradiometer (MODIS) CF data showed significant cloud  
3 cover (up to 0.8 – 0.9). This significant cloud fraction along SAL together with clouds over  
4 the Atlantic Inter-tropical Convergence Zone contributes to the above-mentioned hemispheric  
5 CF asymmetry. Both Multi-Angle Imaging SpectroRadiometer (MISR) measurements and  
6 MERRAero data were in agreement on seasonal variations in hemispheric aerosol asymmetry.  
7 Hemispheric asymmetry in total AOT over the Atlantic was the most pronounced between  
8 March and July, when dust presence over the North Atlantic was maximal. In September and  
9 October, there was no noticeable hemispheric asymmetry in total AOT over the tropical  
10 Atlantic.

11

## 12 **1 Introduction**

13 [Hemispheric asymmetry in cloud fraction \(CF\) and aerosols could lead to hemispheric](#)  
14 [imbalance in solar radiation reaching the surface and, consequently, could affect the Earth's](#)  
15 [climate](#). Satellite observations have been widely used in the study of aerosol optical thickness  
16 and cloud cover because of their capability of providing global coverage on a regular basis.  
17 Previous studies, using different space-borne aerosol sensors, discussed the idea that the  
18 hemispheres are asymmetric in aerosol distribution (Remer et al., 2008; Kaufman et al.,  
19 2005a; Remer and Kaufman, 2006, Mishchenko and Geogdzhayev, 2007, Chou et al., 2002,  
20 Zhang and Reid, 2010, Hsu et al., 2012, Kishcha et al, 2007, 2009). The Advanced Very High  
21 Resolution Radiometer (AVHRR) satellite data over the ocean were used by Mishchenko and  
22 Geogdzhayev (2007) to compare monthly averaged aerosol optical thickness (AOT) over the  
23 Northern and Southern Hemispheres. They found a difference in AOT averaged over the two  
24 hemispheres. Chou et al. (2002) obtained meridional distribution of AOT over the ocean by  
25 using the Sea-viewing Wide Field-of-view Sensor (SeaWiFS) satellite data for the year 1998.  
26 Hsu et al. (2012) displayed the asymmetric spatial distribution of seasonally-averaged  
27 SeaWiFS AOT from 1997 to 2010. Several studies based on the Moderate Resolution  
28 Imaging Spectroradiometer (MODIS) and Multi-Angle Imaging SpectroRadiometer (MISR)  
29 data showed that aerosol parameters are distributed asymmetrically on the two hemispheres  
30 (Remer et al., 2008; Kaufman et al., 2005a; Remer and Kaufman, 2006, Zhang and Reid,  
31 2010, Kishcha et al., 2007, 2009). In our previous study (Kishcha et al., 2009), AOT data  
32 from three satellite sensors (MISR, MODIS-Terra, and MODIS-Aqua) were used in order to

1 analyze seasonal variations of meridional AOT asymmetry over the global ocean. The  
2 asymmetry was pronounced in the April–July months, while there was no noticeable  
3 asymmetry during the season from September to December. Kishcha et al. (2009) mentioned  
4 that not only the Northern Hemisphere but also the Southern Hemisphere contributed to the  
5 formation of noticeable hemispheric aerosol asymmetry. During the season of pronounced  
6 hemispheric aerosol asymmetry, an increase in AOT was observed over the Northern  
7 Hemisphere, while a decrease in AOT was observed over the Southern Hemisphere. It was  
8 found that, over the global ocean, there was no noticeable asymmetry in meridional  
9 distribution of cloud fraction.

10 The Sahara desert emits dust in large quantities over the tropical Atlantic (Prospero and  
11 Lamb, 2003). Previous studies have shown that desert dust particles can influence the Earth's  
12 atmosphere in the following ways: directly by scattering and absorbing solar and thermal  
13 radiation, and indirectly by acting as cloud and ice condensation nuclei (Choobari et al, 2013  
14 and references therein, Pey et al., 2013). It was shown by Wilcox et al. (2010) that the  
15 radiative effect of Saharan dust tends to draw the Atlantic Intertropical Convergence Zone  
16 (ITCZ) northward toward the Saharan Air Layer (SAL). Alpert et al. (1998) discussed the  
17 response of the atmospheric temperature field to the radiative forcing of Saharan dust over the  
18 North Atlantic Ocean. Dust particles over the Atlantic Ocean may essentially influence  
19 tropical cloud systems and precipitation (Kaufman et al., 2005b, Johnson et al., 2004, Min et  
20 al., 2009, Ben-Ami et al., 2009, Feingold et al., 2009, Rosenfeld et al., 2001).

21 To our knowledge, over a limited ocean area, hemispheric asymmetry of aerosols and cloud  
22 fraction relative to the equator has not been investigated so far. We chose the tropical Atlantic  
23 (30°N – 30°S) because it is characterized by significant amounts of Saharan dust. We wished  
24 to find out if the meridional CF distribution remains symmetrical relative to the equator in the  
25 presence of such strong hemispheric aerosol asymmetry. We determined and compared the  
26 contribution of desert dust and that of other aerosol species to aerosol asymmetry between the  
27 tropical North and South Atlantic Oceans. Analyzing the meridional distribution of various  
28 aerosol species over the tropical Atlantic Ocean was carried out using the NASA Aerosol  
29 Reanalysis (aka MERRAero). This reanalysis has been recently developed at NASA's Global  
30 Modeling Assimilation Office (GMAO) using a version of the NASA Goddard Earth  
31 Observing System-5 (GEOS-5) model radiatively coupled with Goddard Chemistry, Aerosol,  
32 Radiation, and Transport (GOCART) aerosols. An important property of GEOS-5 is data

1 assimilation inclusion of bias-corrected aerosol optical thickness from the MODIS sensor on  
2 both Terra and Aqua satellites. Of course, AOT assimilation is effective only for two short  
3 periods of MODIS's appearance over the study area. All other time (18 hours per day) the  
4 GEOS-5 model works independently of MODIS (Kishcha et al., 2014).

5

## 6 **2 GEOS-5 and the MERRA Aerosol Reanalysis (MERRAero)**

7 GEOS-5 is the latest version of the NASA Global Modeling and Assimilation Office  
8 (GMAO) Earth system model, which was used to extend the NASA Modern Era-  
9 Retrospective Analysis for Research and Applications (MERRA) with five atmospheric  
10 aerosol components (sulfates, organic carbon, black carbon, desert dust, and sea-salt). GEOS-  
11 5 includes aerosols based on a version of the Goddard Chemistry, Aerosol, Radiation, and  
12 Transport (GOCART) model (Colarco et al., 2010, Chin et al., 2002). Both dust and sea salt  
13 have wind-speed dependent emission functions (Colarco et al., 2010), while sulfate and  
14 carbonaceous species have emissions principally from fossil fuel combustion, biomass  
15 burning, and bio-fuel consumption, with additional biogenic sources of organic carbon.  
16 Sulfate has additional chemical production from oxidation of SO<sub>2</sub> and dimethylsulfide  
17 (DMS), as well as volcanic SO<sub>2</sub> emissions. Aerosol emissions for sulfate and carbonaceous  
18 species are based on the AeroCom version 2 hindcast inventories  
19 [<http://aerocom.met.no/emissions.html>]. Daily biomass burning emissions are from the Quick  
20 Fire Emission Dataset (QFED) and are derived from MODIS fire radiative power retrievals  
21 (Darmenov and da Silva, 2013). GEOS-5 also includes assimilation of AOT observations  
22 from the MODIS sensor on both Terra and Aqua satellites. The obtained ten-year (July 2002 –  
23 June 2012) MERRA-driven aerosol reanalysis (MERRAero) dataset was applied to the  
24 analysis of hemispheric aerosol asymmetry in the current study. In order to verify the  
25 obtained meridional aerosol distribution based on MERRAero, we used the Multi-angle  
26 Imaging SpectroRadiometer (MISR) monthly global 0.5° x 0.5° AOT dataset available over  
27 the study period.

28

## 29 **3 Method**

30 Over the tropical Atlantic Ocean (30°N – 30°S), variations of zonal-averaged AOT as a  
31 function of latitude were used to analyze meridional aerosol distribution, following our  
32 previous study (Kishcha et al., 2009). This included total AOT and AOT of various aerosol

1 species. To quantify [hemispheric](#) AOT asymmetry, the hemispheric ratio (R) of AOT  
 2 averaged separately over the tropical North Atlantic ( $X_N$ ) to that over the tropical South  
 3 Atlantic ( $X_S$ ) was estimated. The hemispheric ratio is equal to 1 in the case of the two parts  
 4 of the tropical Atlantic holding approximately the same averaged AOT, while the ratio is  
 5 greater (less) than 1 if the North (South) Atlantic dominates the other one. Standard deviation  
 6 of the reported hemispheric ratio (Table 1) was estimated in accordance with the following  
 7 formula by Ku [1966], NIST/SEMATECH (2006):

$$8 \quad C_R = \frac{1}{\sqrt{N}} \cdot \frac{X_N}{X_S} \cdot \sqrt{\frac{C_N^2}{X_N^2} + \frac{C_S^2}{X_S^2} - 2 \cdot \frac{C_{NS}}{X_N \cdot X_S}}$$

9 where  $C_N$ ,  $C_S$  are standard deviations of zonal averaged AOTs in the tropical North and  
 10 South Atlantic Oceans respectively,  $C_{NS}$  is their covariance, and  $N = 120$  stands for the  
 11 number of months in the MISR/ MERRAero AOT monthly data set used.

12 Variations of meridional aerosol distributions were analyzed by using [Version 3.1 of MISR](#)  
 13 [Level 3 AOT measurements](#) and MERRAero data during the 10-year period, from July 2002  
 14 to June 2012. The MISR swath width is about 380 km and global coverage is obtained every 9  
 15 days. MISR AOT has been extensively validated against Aerosol Robotic Network  
 16 (AERONET) Sun photometer measurements over different regions (Martonchik et al., 2004;  
 17 Christopher and Wang, 2004; Kalashnikova and Kahn, 2008; Liu et al., 2004). For the  
 18 purpose of comparing meridional distributions of cloud cover with those of AOT during the  
 19 same 10-year period (July 2002 – June 2012), Collection [5.1](#) of MODIS-Terra Level 3  
 20 monthly daytime cloud fraction (CF) data, with horizontal resolution  $1^\circ \times 1^\circ$  was used  
 21 ([Ackerman et al., 1998](#), [Frey et al., 2008](#), King et al., 2003). Furthermore, to analyze  
 22 meridional rainfall distribution, the Tropical Rainfall Measuring Mission (TRMM) monthly  
 23  $0.25^\circ \times 0.25^\circ$  Rainfall Data Product (3B43 Version 7) was used ([Huffman et al., 2007](#)).  
 24 MODIS CF data and TRMM data were acquired using the GES-DISC Interactive Online  
 25 Visualization and Analysis Infrastructure (Giovanni) as part of NASA Goddard Earth  
 26 Sciences (GES) Data and Information Services Center (DISC) ([Acker and Leptoukh, 2007](#)).

27

## 1 **4 Results**

### 2 **4.1 Ocean zone with the predominance of desert dust aerosols**

3 MERRAero showed that the Sahara desert emits a significant amount of dust into the  
4 atmosphere over the Atlantic Ocean (Fig. 1, a, c, and e). With respect to different oceans,  
5 MERRAero showed that desert dust dominates all other aerosol species only over the Atlantic  
6 Ocean. Fig. 1 (b, d, and f) represents spatial distribution of the ratio of dust AOT to AOT of  
7 all other aerosol species. The red contour lines represent the boundary of the zone where dust  
8 AOT is equal to AOT of all other aerosol species. One can see that, through the 10-year  
9 period under consideration, over the Atlantic Ocean within the latitudinal zone between 7°N  
10 and 30°N, Saharan dust dominates other aerosol species (Fig. 1b). The longitudinal dimension  
11 of this zone is subject to seasonal variability. During the dusty season from March to July, the  
12 zone of dust predominance occupies a significant part of the tropical Atlantic between North  
13 Africa and Central America. Specifically, as shown in Fig. 1d, in July, the zone of dust  
14 predominance is extremely extensive. By contrast, from October to February, this zone is  
15 observed only over some limited territory close to North Africa.

16 Desert dust can be seen not only over the Atlantic Ocean, but also over the Pacific and Indian  
17 Oceans (Fig. 1, a, c, and e). However, outside the Atlantic Ocean, one can see only limited  
18 zones of desert dust predominance over the Mediterranean Sea and over the Arabian Sea (Fig.  
19 1, b, d, and f). Therefore, the tropical North Atlantic Ocean is the largest ocean area where  
20 dust particles determine the atmospheric aerosol content, based on MERRAero data.

21

### 22 **4.2 Meridional distribution of total AOT over the tropical Atlantic Ocean**

23 Figure 2a represents meridional distribution of ten-year mean AOT (July 2002 – June 2012),  
24 zonal averaged over the tropical Atlantic Ocean. One can see that MERRAero showed  
25 similarity to the meridional AOT distribution, based on MISR data (Fig. 2a). Specifically,  
26 MERRAero was able to reproduce the hemispheric asymmetry in the AOT distribution,  
27 including a monomodal maximum in the tropical North Atlantic and a minimum in the  
28 tropical South Atlantic. This monomodal AOT maximum was discussed in our previous study  
29 (Kishcha et al., 2009). Both MISR and MERRAero showed that, in the minimum, the AOT  
30 values were three times lower than those in the maximum. We quantified meridional AOT  
31 asymmetry relative to the equator in the tropical Atlantic Ocean (30°N – 30°S) by obtaining  
32 the hemispheric ratio ( $R_{AOT}$ ) of AOT averaged separately over the tropical North Atlantic to

1 AOT averaged over the tropical South Atlantic:  $R_{AOT}$  was estimated to be about 1.7 (Table 1).  
2 This means that, over the 10-year period under consideration, there were **many more** aerosol  
3 particles over the tropical North Atlantic than over the tropical South Atlantic.

4

### 5 **4.3 Seasonal variations of meridional distribution of AOT**

6 For each month of the year, we analyzed variations of meridional distribution of AOT over  
7 the tropical Atlantic Ocean (Fig. 3). It was found that the meridional AOT distribution is  
8 seasonal dependent. In particular, both MISR and MERRAero were in agreement that the  
9 monomodal AOT maximum, a characteristic feature of hemispheric asymmetry in AOT,  
10 exists but not in each month. In the months from September to October, two AOT maxima  
11 can be observed: one maximum in the North Atlantic, and another one in the South Atlantic.

12 Figure 4 represents month-to-month variations of the hemispheric ratio  $R_{AOT}$  over the tropical  
13 Atlantic for each month of the year. Both MISR and MERRAero showed that meridional  
14 AOT asymmetry was most pronounced during the season from March to July (Fig. 4). One  
15 can see that, from month to month during the year,  $R_{AOT}$  ranges from 1 to 2.4, while during  
16 the season of pronounced hemispheric aerosol asymmetry (March – July)  $R_{AOT}$  ranges from  
17 2.0 – 2.4. In September and October,  $R_{AOT}$  was close to 1, indicating no noticeable asymmetry  
18 (Fig. 4).

19

### 20 **4.4 Meridional distribution of AOT of various aerosol species**

21 Fig. 2c represents meridional distribution of ten-year mean MERRAero AOT for total AOT  
22 (Total), dust AOT (DU), organic and black carbon aerosol AOT (OC & BC), and AOT of  
23 other aerosol species (Other), zonal averaged over the tropical Atlantic Ocean. One can see  
24 that meridional dust distribution is much more asymmetric relative to the equator than  
25 meridional distribution of OC & BC and other aerosol species. The hemispheric asymmetry of  
26 DU, characterized by the hemispheric ratio ( $R_{DU}$ ) of dust AOT was about 11 (Table 2). Such  
27 strong asymmetry in meridional distribution of desert dust over the ocean can be explained by  
28 its transport by winds from the Sahara desert to the ocean in the North Atlantic. Being the  
29 major contributor to the AOT maximum in the North Atlantic, Saharan dust was responsible  
30 for the pronounced meridional AOT asymmetry in total AOT over the tropical Atlantic  
31 Ocean. Carbon aerosols also displayed some hemispheric asymmetry characterized by the  
32 hemispheric ratio  $R_{OC\&BC} = 0.7$ , although this asymmetry was much less pronounced than that

1 of desert dust (Fig. 2c and Table 2). Meridional distribution of AOT of other aerosol species  
2 was almost symmetrical ( $R_{\text{Other}}$  is 1.1) (Table 2). Therefore, aerosols over the tropical Atlantic  
3 can be divided into two groups with different meridional distribution relative to the equator:  
4 dust and carbonaceous aerosols were distributed asymmetrically, while other aerosol species  
5 were distributed **more** symmetrically.

6 MERRAero showed that seasonal variations of transatlantic Saharan dust transport  
7 determined the seasonal variations of meridional dust asymmetry. In May - July, when  
8 hemispheric asymmetry in dust AOT over the tropical North Atlantic was the most  
9 pronounced, dust AOT averaged separately over the tropical North Atlantic was one order of  
10 magnitude higher than dust AOT averaged over the tropical South Atlantic (Table 2). In July,  
11 the most pronounced hemispheric asymmetry of dust AOT was characterized by the  
12 hemispheric ratio  $R_{\text{DU}}$  of about 30 (Table 2).

13 When dust presence over the North Atlantic was minimal, the contribution of other aerosol  
14 species to the meridional distribution of total AOT could be significant. In particular, in  
15 December, the maximum in OC & BC at low-latitudes (due to the transport of bio-mass  
16 burning smoke) contributed significantly to the maximum in total AOT in the tropical North  
17 Atlantic (Fig. 5a). Note that the reason for the aforementioned transport of bio-mass burning  
18 aerosols is the burning of agricultural waste in the Sahelian region of northern Africa. This  
19 burning activity is maximal during December – February (Haywood et al., 2008). MERRAero  
20 showed that no noticeable hemispheric asymmetry of total AOT was observed in September  
21 and October (Fig. 4). This is because the contribution of carbonaceous aerosols (OC & BC) to  
22 total AOT over the South Atlantic is approximately equal to the contribution of Saharan dust  
23 to total AOT in the North Atlantic (Fig. 5). The reason for the observed increase in OC & BC  
24 over the South Atlantic in September and October is that these months fall within the burning  
25 period in Central Africa, where slash-and-burn agriculture is prevalent (Tereszchuk et al.,  
26 2011). In September and October, AOT of carbonaceous aerosols over the tropical South  
27 Atlantic was five times higher than that over the tropical North Atlantic ( $R_{\text{OC\&BC}} = 0.2$ ) (Table  
28 2).

29 Meridional distribution of AOT of other aerosol species remains more symmetrical than dust  
30 and carbonaceous aerosols throughout all months (the hemispheric ratio  $R_{\text{Other}}$  ranged from  
31 0.8 – 1.3) (Table 2). This group includes marine aerosols, such as sea-salt and dimethylsulfide  
32 (DMS) aerosols, which are produced everywhere in the tropical Atlantic Ocean.

1

## 2 **4.5 Meridional distribution of cloud fraction**

3 We analyzed meridional distribution of cloud cover over the tropical (30°N – 30°S) Atlantic  
4 Ocean, which includes the area of transatlantic Saharan dust transport within SAL. Fig. 2b  
5 represents the meridional distribution of 10-year mean cloud fraction, zonal averaged over the  
6 Atlantic Ocean. One can see the local maximum near the equator due to clouds concentrated  
7 over the Intertropical Convergence Zone: this maximum shifts to the north from the equator.  
8 Despite this CF maximum, the hemispheric CF ratio ( $R_{CF}$ ), characterized by the ratio of CF  
9 averaged separately over the tropical North and over the South Atlantic, did not exceed 1.1  
10 (Table 1).

11 As mentioned in Sect. 4.4, MERRAero showed that dust and carbonaceous aerosols were  
12 distributed asymmetrically in relation to the equator, while other aerosol species were  
13 distributed more symmetrically. During the period of pronounced meridional AOT  
14 asymmetry over the tropical Atlantic from May - July, dust AOT averaged separately over the  
15 tropical North Atlantic was about one order of magnitude higher than dust AOT averaged  
16 over the tropical South Atlantic (Table 2). In July, the hemispheric ratio  $R_{DU}$  was roughly 30.  
17 In the presence of such strong meridional dust asymmetry, in July,  $R_{CF}$  reached 1.2 (Table 2  
18 and Fig. 4). As shown in previous study (Kishcha et al., 2009), over the global ocean,  $R_{AOT}$   
19 was about 1.5, while  $R_{CF}$  was 1. Therefore, by contrast to the global ocean (where meridional  
20 CF distribution was symmetrical over the two hemispheres), over the tropical Atlantic in July,  
21 CF averaged separately over the tropical North Atlantic exceeded CF averaged over the  
22 tropical South Atlantic by 20%. In September – October, when there was no hemispheric  
23 asymmetry in total AOT over the tropical Atlantic ( $R_{AOT}$  was close to 1), meridional CF  
24 distribution was also almost symmetrical ( $R_{CF}$  was equal to 1, (Table 2 and Fig. 4)).

25 Fig. 6 represents meridional distribution of MODIS CF and TRMM accumulated rainfall,  
26 zonal averaged over the tropical Atlantic Ocean, for all months of the year. One can see some  
27 changes in CF from month to month on the high background level of approximately 0.6. This  
28 background level of CF is almost the same over the tropical North and South Atlantic Oceans.

29 In each month, the main CF maximum coincides with the Atlantic Ocean inter-tropical  
30 convergence zone, which is characterized by intensive rainfall (Fig. 6). In the summer months  
31 (when pronounced meridional dust asymmetry was observed), MODIS CF data showed  
32 significant CF to the north from the main CF maximum, over the latitudes of transatlantic dust



1 transport within the Saharan Air Layer (SAL) (Fig. 6, g to i). Saharan dust travels across the  
2 Atlantic Ocean within the hot and dry Saharan Air Layer (Dunion and Velden, 2004). The  
3 SAL's base is at ~900 – 1800 m and the top is usually below 5500 m (Diaz et al., 1976). The  
4 significant cloud fraction along SAL, together with the Atlantic Inter-tropical Convergence  
5 Zone (centered over the tropical North Atlantic) contributed to the above-mentioned  
6 hemispheric CF asymmetry. Following is our analysis of cloud fraction in the area of the  
7 Saharan Air Layer in July, when the most pronounced meridional dust asymmetry was  
8 observed.

9

#### 10 **4.5.1 Cloud fraction in the area of the Saharan Air Layer in July**

11 Figure 7 represents meridional distribution of the 10-year mean of MERRAero dust AOT,  
12 MODIS-Terra cloud fraction, and TRMM accumulated rainfall, zonal averaged over the  
13 Atlantic Ocean (60°W – 0°E). The near-equatorial maximum in meridional distribution of  
14 TRMM accumulated rainfall indicates the position of the North Atlantic Ocean inter-tropical  
15 convergence zone (ITCZ) (Fig. 7). One can see that, in July, when dust presence over the  
16 Atlantic is maximal, the meridional distribution of CF becomes essentially asymmetric with  
17 respect to the center of ITCZ. In particular, significant CF up to 0.8 is seen [to the North of](#)  
18 ITCZ, over the latitudes with SAL presence (12°N – 24°N) (Fig. 7). These values are higher  
19 than the 10-year mean MODIS CF over the tropical North Atlantic (0.66) (Table 1). One can  
20 consider that, in the North Atlantic, the wide maximum in the meridional distribution of CF  
21 consists of two different partly-overlapping maxima: one CF maximum located within ITCZ,  
22 and the other CF maximum located [to the north of ITCZ](#), over the ocean area where Saharan  
23 dust is transported within the SAL across the Atlantic (Fig. 7).

24 More detailed information about the aforementioned two partly-overlapping maxima in the  
25 meridional distribution of CF in July can be obtained from a comparison between spatial  
26 distribution of 10-year mean MERRAero dust AOT and MODIS CF over the tropical North  
27 Atlantic (Fig. 8, a and b). It is clearly seen that the ocean area with Saharan dust transported  
28 across the Atlantic is covered by cloudiness characterized by significant values of MODIS CF  
29 up to 0.8 – 0.9. This CF is higher than the 10-year mean MODIS CF over the tropical North  
30 Atlantic (0.66) (Table 1). Note that there is a strong difference between the two zones of  
31 significant CF in the North Atlantic. High values of CF within ITCZ are accompanied by

1 intensive rainfall (Fig. 8, b and c). By contrast, the area of SAL with significant CF (12°N –  
2 24°N) is characterized by essentially lower precipitation (Fig. 8, b and c).

3 To quantify changes in dust AOT, MODIS-based CF, and TRMM monthly-accumulated  
4 rainfall with distance from the Sahara, we analyzed the 10-year mean (July 2002 – June 2012)  
5 of these parameters over six zones, each 6° x 6°, located along the Saharan Air Layer, in  
6 accordance with the direction of dust transport (Fig. 8a). In July, there was a decrease of  
7 approximately 300% in dust AOT from zone 1 to zone 6 (Fig. 9a). The reason for the  
8 decrease in dust AOT with increasing distance from dust sources in the Sahara is gravitational  
9 settling of dust particles (mainly coarse fraction). As shown in Figs. 9 a and b, the strong  
10 decrease in dust AOT from zone 1 to zone 3 was not accompanied by any changes in TRMM  
11 accumulated rainfall. Therefore, the washing out of aerosols by rainfall does not account for  
12 the aerosol spatial decrease with distance from the Sahara. Consequently, it proves that  
13 gravitational settling of dust particles accounts for the aerosol spatial decrease with distance  
14 from the Sahara.

15 MODIS cloud fraction also decreased from zone 1 to zone 3, although less pronounced than  
16 dust (Fig. 9b). Over zones 1 – 3, there was significant cloud fraction in the presence of limited  
17 precipitation less than 20 mm month<sup>-1</sup>. This indicates that clouds in zones 1 – 3 were not  
18 developed enough to produced intensive precipitation. This can be explained by the effect of  
19 temperature inversion below the SAL base on cloud formation (Prospero and Carlson, 1972).

20 To examine temperature inversion over the specified zones, we analyzed vertical profiles of  
21 10-year mean MERRA Reanalysis atmospheric temperature in July, averaged over the  
22 specified zones. As shown in Fig. 10, the temperature inversion existed over zones 1 – 4, and  
23 it disappeared over zones 5 and 6. The observed temperature inversion over zones 1 to 4 (Fig.  
24 10) prevented deep cloud formation, which explains the observed limited precipitation in  
25 these zones (Fig. 9b). In the absence of temperature inversion over zones 5 and 6 (Fig. 10),  
26 one can consider the presence of developed clouds, which were capable of producing  
27 intensive rainfall. Such developed clouds could explain the observed precipitation up to 110  
28 mm month<sup>-1</sup> over zones 5 – 6 (Fig. 9b).

29

#### 30 **4.5.2 Influence of dust loading on CF in the area of SAL**

31 The observed temperature inversion over zones 1 - 4 prevents deep cloud formation; this  
32 explains limited precipitation in these zones. On the other hand, meteorological conditions

1 below the temperature inversion at the SAL base include significant atmospheric humidity  
2 and the presence of large amounts of settling dust particles together with marine aerosols.

3 As known, aerosol species often combine to form mixed particles, with properties different  
4 from those of their components (Andreae et al., 2009). Mineral dust particles are known to be  
5 not very efficient cloud condensation nuclei (CCN), unless they are coated with soluble  
6 materials (Andreae et al., 2009). Using airplane measurements, Levin et al. (2005) showed  
7 that dust transport over the sea could lead to sea-salt coating on dust particles. Coating settling  
8 dust particles with sea-salt could modify them into efficient CCN. Being below the  
9 temperature inversion and acting as efficient CCN, Saharan dust particles coated with soluble  
10 material contribute to the formation of shallow stratocumulus clouds. This physical  
11 mechanism, based on the indirect effect of Saharan dust on stratocumulus clouds below the  
12 temperature inversion, could explain the observed significant cloud cover (CF up to 0.8 – 0.9)  
13 along the Saharan Air Layer. The significant cloud fraction along SAL contributes to  
14 hemispheric CF asymmetry over the tropical Atlantic. This could lead to hemispheric  
15 imbalance in strong solar radiation reaching the sea surface in the tropical Atlantic Ocean.

16 To examine the properties of clouds in the area of SAL, we analyzed available data on the  
17 effective radius of cloud droplets. Fig. 11 represents histograms of the effective radius ( $R_{eff}$ )  
18 of cloud droplets for liquid water clouds in the specified zones 1 – 4 along SAL, based on  
19 MODIS L3 gridded monthly data ( $1^\circ \times 1^\circ$ ) during the 10-year study period in July. The data  
20 were supplied by the Giovanni data base. It is obvious that the cloud droplet effective radius  
21 increases from zone 1 to zone 4 (Fig. 11). One can see a systematic shift in the whole  
22 histogram to higher values of  $R_{eff}$  from zone 1 to zone 4. This can be explained by the  
23 decrease in CCN numbers associated with the decreasing numbers of settling Saharan dust  
24 particles with distance from the Sahara, in accordance with the decrease in dust AOT shown  
25 in Fig. 9a.

26 Thus, the cloud droplet effective radius in zone 4 was larger than in zones 1 - 3. This could  
27 lead to some increase in precipitation in zone 4. Indeed, as shown in Fig. 9b, TRMM  
28 accumulated rainfall in zone 4 was more intensive than over zones 1 - 3. This supports the  
29 above-mentioned physical mechanism of cloud formation below the temperature inversion at  
30 the SAL base.

31 In accordance with the above-mentioned mechanism of cloud formation along SAL, there are  
32 different cloud types over zones 1 – 4 on the one hand, and over zones 5 – 6 on the other

1 hand. Over zones 1 – 4, we consider the presence of shallow stratocumulus clouds below the  
2 temperature inversion at the SAL base. These shallow stratocumulus clouds are characterized  
3 by limited precipitation. Over zones 5 – 6, we consider the presence of developed clouds  
4 capable of producing strong precipitation up to 110 mm month<sup>-1</sup>.

### 6 **4.5.3. Possible MODIS CF contamination by heavy dust loading**

7 Collection 5 of MODIS-Terra monthly daytime cloud fraction data used in the current study  
8 are derived from the standard cloud mask product based on the cloud mask algorithm MOD35  
9 (Ackerman et al., 1998, Frey et al., 2008). In heavy dust loading situations, such as dust  
10 storms over deserts, MOD35 may flag the aerosol-laden atmosphere as cloudy (Ackerman et  
11 al., 1998).

12 During dust storms over deserts, observed AOT values range from 2 to 5 (e.g. Alam et al.,  
13 2014). However, over the tropical North Atlantic in July, strong AOT exceeding even 1 is a  
14 very rare phenomenon. To demonstrate that AOT exceeding 1 is a rare phenomenon over the  
15 tropical North Atlantic, Fig. 12a represents a histogram of AOT observed over the tropical  
16 North Atlantic in July, 2010, based on MODIS Level 3 AOT daily data. July 2010 was chosen  
17 because AOT, averaged over the tropical North Atlantic, was maximal compared to AOT in  
18 other July months, during the 10-year study period. One can see that AOT hardly exceeded 1.  
19 A similar situation can be seen over the latitudes with SAL presence (12°N – 24°N) (Fig.  
20 12b). Therefore, the effect of MODIS cloud fraction contamination by heavy dust loading  
21 cannot essentially contribute to averaging CF over the tropical North Atlantic. Consequently,  
22 given the large amount of available MODIS CF daily data over the 10-year study period,  
23 cloud fraction contamination does not account for the obtained hemispheric CF asymmetry  
24 over the tropical Atlantic Ocean.

## 26 **5 Conclusions**

27 Meridional distribution of aerosol optical thickness and cloud fraction were analyzed using  
28 10-year satellite measurements from MISR and MODIS, together with MERRAero data (July  
29 2002 – June 2012). In the current study, we focus on the tropical Atlantic (30°N – 30°S)  
30 which is characterized by significant amounts of Saharan dust dominating other aerosol  
31 species over the North Atlantic.

1 Our main point is that, over the tropical Atlantic, not only is Saharan dust responsible for the  
2 pronounced hemispheric aerosol asymmetry, but it also contributes to significant cloud cover  
3 along the Saharan Air Layer. This could lead to the hemispheric imbalance in strong solar  
4 radiation reaching the sea surface in the tropical Atlantic.

5 When hemispheric AOT asymmetry over the tropical North Atlantic was the most  
6 pronounced, dust AOT averaged separately over the tropical North Atlantic was one order of  
7 magnitude higher than that over the tropical South Atlantic. In July, the most pronounced  
8 hemispheric asymmetry of dust AOT was characterized by the hemispheric ratio  $R_{DU}$  of  
9 approximately 30. In the presence of such strong hemispheric asymmetry in dust AOT in the  
10 summer months, CF averaged separately over the tropical North Atlantic exceeded CF  
11 averaged over the tropical South Atlantic by 20%.

12 In July, along the Saharan Air Layer, MODIS CF data showed cloud cover up to 0.8 – 0.9  
13 with limited precipitation ability. These CF values are higher than the 10-year mean MODIS  
14 CF over the tropical North Atlantic (0.66) (Table 1). The observed significant cloud fraction  
15 along SAL could be explained by the formation of shallow stratocumulus clouds below the  
16 temperature inversion at the SAL base with the assistance of settling Saharan dust particles.  
17 This cloud fraction along SAL together with clouds over the Atlantic Inter-tropical  
18 Convergence Zone contributes to the above-mentioned hemispheric CF asymmetry between  
19 the tropical North and South Atlantic.

20 With respect to different oceans, only over the Atlantic Ocean did MERRAero demonstrate  
21 that desert dust dominated all other aerosol species and was responsible for hemispheric  
22 aerosol asymmetry there. MERRAero showed that, over the tropical Atlantic, dust and  
23 carbonaceous aerosols were distributed asymmetrically relative to the equator, while other  
24 aerosol species were distributed more symmetrically.

25 Both MISR measurements and MERRAero data were in agreement on seasonal variations in  
26 hemispheric aerosol asymmetry. Hemispheric asymmetry in total AOT over the Atlantic was  
27 the most pronounced between March and July, when dust presence over the North Atlantic  
28 was maximal. In September and October, there was no noticeable hemispheric aerosol  
29 asymmetry in total AOT ( $R_{AOT}$  was close to 1). During these two months, the contribution of  
30 carbonaceous aerosols to total AOT in the South Atlantic was comparable to the contribution  
31 of dust aerosols to total AOT in the North Atlantic. Our study showed that, in September and

1 October, meridional CF distribution over the tropical Atlantic was almost symmetrical ( $R_{CF}$   
2 was close to 1).

3

#### 4 **Acknowledgements**

5 We acknowledge the GES-DISC Interactive Online Visualization and Analysis Infrastructure  
6 (Giovanni) for providing us with MODIS and TRMM data. Dr. Long acknowledges support  
7 from the Office of Biological and Environmental Research of the U.S. Department of Energy  
8 as part of the Atmospheric Systems Research Program. The Tel-Aviv University team  
9 acknowledges support from the international Virtual Institute DESERVE (Dead Sea Research  
10 Venue), funded by the German Helmholtz Association.

11

12

## 1 **References**

- 2 Acker, J.G., and Leptoukh, G.: Online analysis enhances use of NASA Earth science data,  
3 Eos Trans. AGU, 88(2), 14 – 17, doi:10.1029/2007EO020003, 2007.
- 4 Ackerman, S.A., Strabala, K.I., Menzel, W.P., Frey, R.A., Moeller, C.C., and Gumley, L.E.:  
5 Discriminating clear sky from clouds with MODIS, J. Geophys. Res., 103(D24), 32141–  
6 32157, doi:10.1029/1998JD200032, 1998.
- 7 Alam, K., Trautmann, T., Blaschke, T., Subhand, F.: Changes in aerosol optical properties  
8 due to dust storms in the Middle East and Southwest Asia, Remote Sensing of Environment,  
9 143, 216–227, 2014.
- 10 Alpert, P., Kaufman, Y.J., Shay-El, Y., Tanre, D., da Silva, A., Schubert, S., and Joseph, J.H.:  
11 Quantification of dust-forced heating of the lower troposphere. Nature 395, 367-370, 1998.
- 12 Andreae, M.O., Hegg, D.A., and Baltensperger, U.: Sources and nature of atmospheric  
13 aerosols. In Aerosol pollution impact on precipitation. Eds.: Z. Levin and W. Cotton.  
14 Springer, Chapter 3, 45 – 90, 2009.
- 15 Ben-Ami, Y., Koren, I., and Altaratz, O.: Patterns of North African dust transport over the  
16 Atlantic: winter vs. summer, based on CALIPSO first year data. Atmos. Chem. Phys., 9,  
17 7867–7875, 2009.
- 18 Chin, M., Ginoux, P., Kinne, S., Torres, O., Holben, B., Duncan, B.N., Martin, R.V., Logan,  
19 J., Higurashi, A., Nakajima, T.: Tropospheric aerosol optical thickness from the GOCART  
20 model and comparisons with satellite and sun photometer measurements. J. Atmos. Phys. 59,  
21 461–483, doi: [http://dx.doi.org/10.1175/1520-0469\(2002\)059](http://dx.doi.org/10.1175/1520-0469(2002)059), 2002.
- 22 Colarco, P., da Silva, A., Chin, M., and Diehl, T.: Online simulations of global aerosol  
23 distributions in the NASA GEOS-4 model and comparisons to satellite and ground-based  
24 aerosol optical depth. J. Geophys. Res., 115, D14207, doi:10.1029/2009JD012820, 2010.
- 25 Choobari, O.A., Zawar-Reza, P., and Sturman, A.: The global distribution of mineral dust and  
26 its impacts on the climate system: A review. Atmospheric Research, 138, 152-165,  
27 <http://dx.doi.org/10.1016/j.atmosres.2013.11.007>, 2013.
- 28 Chou, M.-D., Chan, P.-K and Wang, M.: Aerosol radiative forcing derived from SeaWiFS-  
29 Retrieved aerosol optical properties. J. Atmos. Sci. (Global Aerosol Climatology special  
30 issue), 59, 748-757, 2002.

1 Christopher, S., and Wang, J.: Intercomparison between multi-angle Imaging  
2 SpectroRadiometer (MISR) and sunphotometer aerosol optical thickness in dust source  
3 regions of China, implications for satellite aerosol retrievals and radiative forcing  
4 calculations. *Tellus B*, 56, 451–456, 2004.

5 Darmenov, A., and da Silva, A.: The quick fire emissions dataset (QFED) - Documentation of  
6 versions 2.1, 2.2 and 2.4. NASA Technical Report Series on Global Modeling and Data  
7 Assimilation. NASA TM-2013-104606, 32, 183p, NASA, Greenbelt, MD, 2013.

8 Diaz, H.F., Carlson, T.N., and Prospero, J.M.: A study of the structure and dynamics of the  
9 Saharan air layer over the northern equatorial Atlantic during BOMEX, NOAA Tech Memo  
10 ERL WMPO-32, 61 pp., NOAA, Silver Spring, Md., 1976.

11 Dunion, J.P., and Velden, C.S.: The impact of the Saharan air layer on Atlantic tropical  
12 cyclone activity, *Bull. Am. Meteorol. Soc.*, 85(3), 353– 365, doi:10.1175/BAMS-85-3-353,  
13 2004.

14 Feingold, G., Cotton, W., Lohmann, U., and Levin, Z.: Effects of pollution aerosols and  
15 biomass burning on clouds and precipitation: numerical modeling studies. In *Aerosol  
16 pollution impact on precipitation*. Eds.: Z. Leven and W. Cotton. Springer, Chapter 7, 243 –  
17 278, 2009.

18 Frey, R.A., Ackerman, S.A., Liu, Y., Strabala, K.I., Zhang, H., Key, J.R., Wang, X.: Cloud  
19 detection with MODIS. Part I: Improvements in the MODIS cloud mask for Collection 5. *J.  
20 Atmos. Ocean. Tech.*, 25, 1057 – 1072, 2008.

21 Haywood, J.M., Pelon, J., Formenti, P., Bharmal, N., Brooks, M., Capes, G., Chazette, P.,  
22 Chou, C., Christopher, S., Coe, H., Cuesta, J., Derimian, Y., Desboeufs, K., Greed, G.,  
23 Harrison, M., Heese, B., Highwood, E.J., B. Johnson, B., Mallet, M., Marticorena, B.,  
24 Marsham, J., Milton, S., Myhre, G., Osborne, S.R., Parker, D.J., Rajot, J.-L., Schulz, M.,  
25 Slingo, A., Tanre, D., P. Tulet, P.: Overview of the Dust and Biomass-burning Experiment  
26 and African Monsoon Multidisciplinary Analysis Special Observing Period-0. *J. Geophys.  
27 Res.*, 113, D00C17, doi:10.1029/2008JD010077, 2008.

28 Hsu, N.C., Gautam, R., Sayer, A.M., Bettenhausen, C., Li, C., Jeong, M.J., Tsay, S.C., and  
29 Holben, B.: Global and regional trends of aerosol optical depth over land and ocean using  
30 SeaWiFS measurements from 1997 to 2010. *Atmos. Chem. Phys.*, 12, 8037-8053,  
31 doi:10.5194/acp-12-8037-2012, 2012.



1 Huffman, G.J., Adler, R.F., Bolvin, D.T., Gu, G., Nelkin, E.J., Bowman, K.P., Hong, Y.,  
2 Stocker, E.F., Wolff, D.B.: The TRMM multisatellite precipitation analysis (TMPA): quasi-  
3 global, multiyear, combined-sensor precipitation estimates at fine scales. *J.*  
4 *Hydrometeorology*, 8, 38 – 55, doi: 10.1175/JHM560.1, 2007.

5 Johnson, B.T., Shine, K.P. and Forster, P.M.: The semi-direct aerosol effect: impact of  
6 absorbing aerosols on marine stratocumulus. *Q.J.R. Meteorol. Soc.*, 130, 1407 – 1422, 2004.

7 Kalashnikova, O.V. and Kahn, R.: Mineral dust plume evolution over the Atlantic from MISR  
8 and MODIS aerosol retrievals. *J. Geophys. Res.*, 113, D24204, doi:10.1029/2008JD010083,  
9 2008.

10 Kaufman, Y.J., Boucher, O., Tanre, D., Chin, M., Remer, L.A. and Takemura, T.: Aerosol  
11 anthropogenic component estimated from satellite data, *Geophys. Res. Lett.*, 32, L17804,  
12 doi:10.1029/2005GL023125, 2005a.

13 Kaufman, Y.J., Koren, I., Remer, L., Rosenfeld, D., and Rudich, Y.: The effect of smoke,  
14 dust, and pollution aerosol on shallow cloud development over the Atlantic Ocean. *Proc. Natl.*  
15 *Acad. Sci. U.S.A.*, 102, 11,207-11,212, 2005b.

16 King, M.D., Menzel, W.P., Kaufman, Y.J., Tanre, D., Gao, B.C., Platnick, S., Ackerman,  
17 S.A., Remer, L.A., Pincus, R. and Hubanks, P.A.: Cloud and aerosol properties, precipitable  
18 water, and profiles of temperature and humidity from MODIS. *IEEE Transactions on*  
19 *Geoscience and Remote Sensing*, 41(2), 442-458, 2003.

20 Kishcha, P., Starobinets, B., and Alpert, P.: Latitudinal variations of cloud and aerosol optical  
21 thickness trends based on MODIS satellite data. *Geophys. Res. Lett.*, 34, L05810,  
22 doi:10.1029/2006GL028796, 2007.

23 Kishcha, P., Starobinets, B., Kalashnikova, O., Long, C.N., and Alpert, P.: Variations in  
24 meridional aerosol distribution and solar dimming. *J. Geophys. Res.*, 114, D00D14,  
25 doi:10.1029/2008JD010975, 2009.

26 Kishcha, P., da Silva, A.M., Starobinets, B., and Alpert, P.: Air pollution over the Ganges  
27 basin and north-west Bay of Bengal in the early post-monsoon season based on NASA  
28 MERRAero data. *J. Geophys. Res. Atmos.*, 119, 1555–1570, doi:10.1002/2013JD020328,  
29 2014.

1 Ku, H.: Notes on the use of propagation of error formulas. *J. Research of National Bureau of*  
2 *Standards – C. Engineering and Instrumentation*, 70C, No.4, 263-273, 1966.

3 Levin, Z., Teller, A., Ganor, E., and Yin, Y.: On the interactions of mineral dust, sea-salt  
4 particles, and clouds: A measurement and modeling study from the Mediterranean Israeli  
5 Dust Experiment campaign, *J. Geophys. Res.*, 110, D20202, doi:10.1029/2005JD005810,  
6 2005.

7 Liu, Y., Sarnat, J.A., Coull, B.A., Koutrakis, P. and Jacob, D.J.: Validation of Multiangle  
8 Imaging Spectroradiometer (MISR) aerosol optical thickness measurements using Aerosol  
9 Robotic Network (AERONET) observations over the contiguous United States. *J. Geophys.*  
10 *Res.*, 109, D06205, doi:10.1029/2003JD003981, 2004.

11 Min, Q.I., Li, R., Lin, B., Joseph, F., Wang, S., Hu, Y., Morris, V., and Chang, F.: Evidence  
12 of mineral dust altering cloud microphysics and precipitation. *Atmos. Chem. Phys.*, 9, 3223-  
13 3231, doi:10.5194/acp-9-3223-2009, 2009.

14 Matronchik, J.V., Diner, D.J., Kahn, R., and Gaitley, B.: Comparison of MISR and  
15 AERONET aerosol optical depths over desert sites. *Geophys. Res. Lett.*, 31, L16102,  
16 doi:10.1029/2004GL019807, 2004.

17 Mishchenko, M.I., and Geogdzhayev, I.V.: Satellite remote sensing reveals regional  
18 tropospheric aerosol trends. *Opt. Express*, 15, 7423 – 7438, doi:10.1364/OE.15.007423, 2007.

19 NIST/SEMATECH e-Handbook of Statistical Methods: available at:  
20 [http://www.itl.nist.gov/25 div898/handbook/](http://www.itl.nist.gov/25%20div898/handbook/) (last access: 07 September 2014), 2006.

21 Pey, J., Querol, X., Alastuey, A., Forastiere, F., and Stafoggia, M.: African dust outbreaks  
22 over the Mediterranean Basin during 2001–2011: PM10 concentrations, phenomenology and  
23 trends, and its relation with synoptic and mesoscale meteorology. *Atmos. Chem. Phys.*, 13,  
24 1395–1410, doi:10.5194/acp-13-1395-2013, 2013.

25 Prospero, J., and Carlson, T.: Vertical and areal distribution of Saharan dust over the Western  
26 Equatorial North Atlantic Ocean. *J. Geophys. Res.*, 77, 5255 – 5265,  
27 doi:10.1029/JC077i027p05255, 1972.

28 Prospero, J., and Lamb, J.: African droughts and dust transport to the Caribbean: climate  
29 change and implications. *Science*, 302, 1024-1027, doi:10.1126/science.1089915, 2003.

1 Remer, L.A. and Kaufman, Y.J.: Aerosol direct radiative effect at the top of the atmosphere  
2 over cloud free ocean derived from four years of MODIS data. *Atmos. Chem. Phys.*, 6, 237-  
3 253, 2006.

4 Remer, L.A., Kleidman, R.G., Levy, R.C., Kaufman, Y.J., Tanre, D., Mattoo, S., Martins,  
5 J.V., Ichoku, C., Koren, I., Hongbin, Yu, Holben, B.N.: Global aerosol climatology from the  
6 MODIS satellite sensors. *J. Geophys. Res.*, 113, D14S07, doi:10.1029/2007JD009661, 2008.

7 Rosenfeld, D., Rudich, Y., Lahav, R.: Desert dust suppressing precipitation - a possible  
8 desertification feedback loop. *Proceedings of the National Academy of Sciences*, 98, 5975-  
9 5980, 2001.

10 Tereszchuk, K.A., Gonz'alez Abad1, G., Clerbaux, C., Hurtmans, D., Coheur, P.F., and P.F.  
11 Bernath, P.F.: ACE-FTS measurements of trace species in the characterization of biomass  
12 burning plumes. *Atmos. Chem. Phys.*, 11, 12169–12179, doi:10.5194/acp-11-12169-2011,  
13 2011.

14 Wilcox, E.M., Lau, K.M., and Kim, K.M.: A northward shift of the North Atlantic Ocean  
15 Intertropical Convergence Zone in response to summertime Saharan dust outbreaks, *Geophys.*  
16 *Res. Lett.*, 37, L04804, doi:10.1029/2009GL041774, 2010.

17 Zhang, J.L. and Reid, J.S.: A decadal regional and global trend analysis of the aerosol optical  
18 depth using a data-assimilation grade over-water MODIS and Level 2 MISR aerosol products.  
19 *Atmos. Chem. Phys.*, 10, 10949-10963, doi:10.5194/acp-10-10949-2010, 2010.

20

1 Table 1. Average AOT and CF over the tropical North ( $X_N$ ) and South ( $X_S$ ) Atlantic and their  
2 hemispheric ratio ( $R$ )<sup>a</sup>. 10-year MERRAero AOT, MISR AOT, and MODIS CF data were  
3 used.

Data set	$X_N \pm \sigma_N$	$X_S \pm \sigma_S$	$R \pm \sigma_R$
MISR AOT	$0.25 \pm 0.06$	$0.15 \pm 0.05$	$1.70 \pm 0.06$
MERRAero AOT	$0.19 \pm 0.05$	$0.12 \pm 0.05$	$1.61 \pm 0.06$
MODIS CF	$0.66 \pm 0.09$	$0.61 \pm 0.06$	$1.08 \pm 0.01$

4 <sup>a</sup>Standard deviations of  $X_N$ ,  $X_S$ , and  $R$  are designated by  $\sigma_N$ ,  $\sigma_S$ ,  $\sigma_R$  respectively.

5

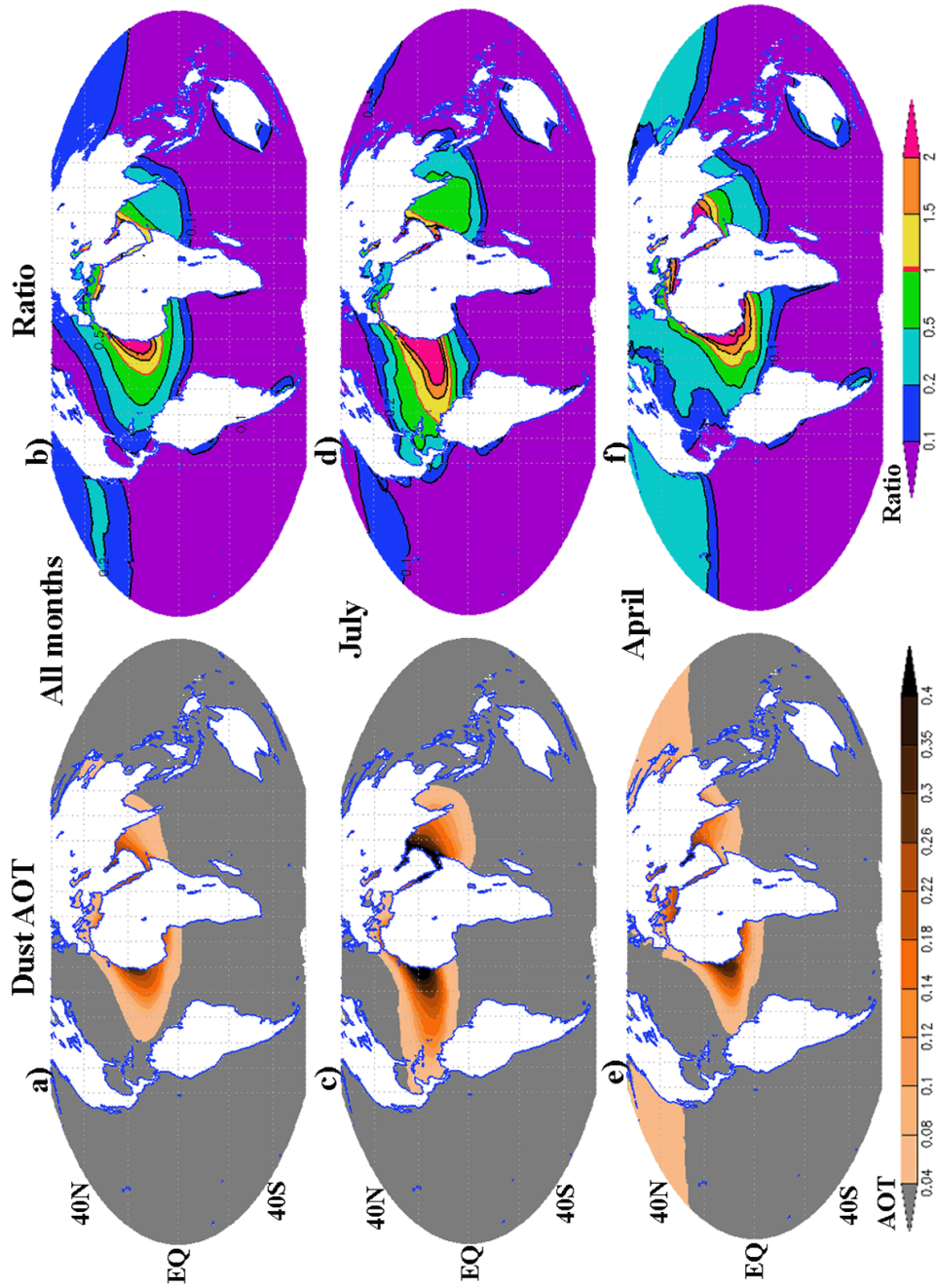
1 Table 2. The hemispheric ratio ( $\pm$  standard deviation) of dust AOT (DU), organic and black  
 2 carbon AOT (OC & BC), other aerosol species AOT (Other), and MODIS CF over the  
 3 tropical Atlantic Ocean (30°N – 30°S). 10-year MERRAero data and MODIS CF data were  
 4 used.

Month	DU	OC & BC	Other	MODIS CF
All months	11.50 $\pm$ 1.20	0.70 $\pm$ 0.10	1.10 $\pm$ 0.10	1.08 $\pm$ 0.01
January	6.10 $\pm$ 2.30	1.30 $\pm$ 0.50	1.10 $\pm$ 0.10	1.10 $\pm$ 0.07
February	4.20 $\pm$ 1.80	1.20 $\pm$ 0.40	1.20 $\pm$ 0.10	1.15 $\pm$ 0.09
March	6.90 $\pm$ 3.20	2.00 $\pm$ 0.40	1.20 $\pm$ 0.10	1.14 $\pm$ 0.10
April	8.80 $\pm$ 4.10	2.70 $\pm$ 0.40	1.20 $\pm$ 0.10	1.07 $\pm$ 0.09
May	21.00 $\pm$ 10.10	1.70 $\pm$ 0.30	1.20 $\pm$ 0.10	1.14 $\pm$ 0.07
June	23.50 $\pm$ 10.80	0.90 $\pm$ 0.30	1.30 $\pm$ 0.10	1.20 $\pm$ 0.09
July	29.30 $\pm$ 10.30	0.70 $\pm$ 0.30	1.30 $\pm$ 0.20	1.21 $\pm$ 0.08
August	25.00 $\pm$ 8.50	0.40 $\pm$ 0.10	1.10 $\pm$ 0.10	1.04 $\pm$ 0.07
September	23.80 $\pm$ 6.70	0.20 $\pm$ 0.10	0.90 $\pm$ 0.10	0.98 $\pm$ 0.05
October	17.00 $\pm$ 4.30	0.20 $\pm$ 0.10	0.80 $\pm$ 0.10	0.97 $\pm$ 0.05
November	9.70 $\pm$ 2.30	0.70 $\pm$ 0.20	0.80 $\pm$ 0.10	0.98 $\pm$ 0.05
December	6.80 $\pm$ 1.90	1.00 $\pm$ 0.30	0.90 $\pm$ 0.10	1.05 $\pm$ 0.05

5

6

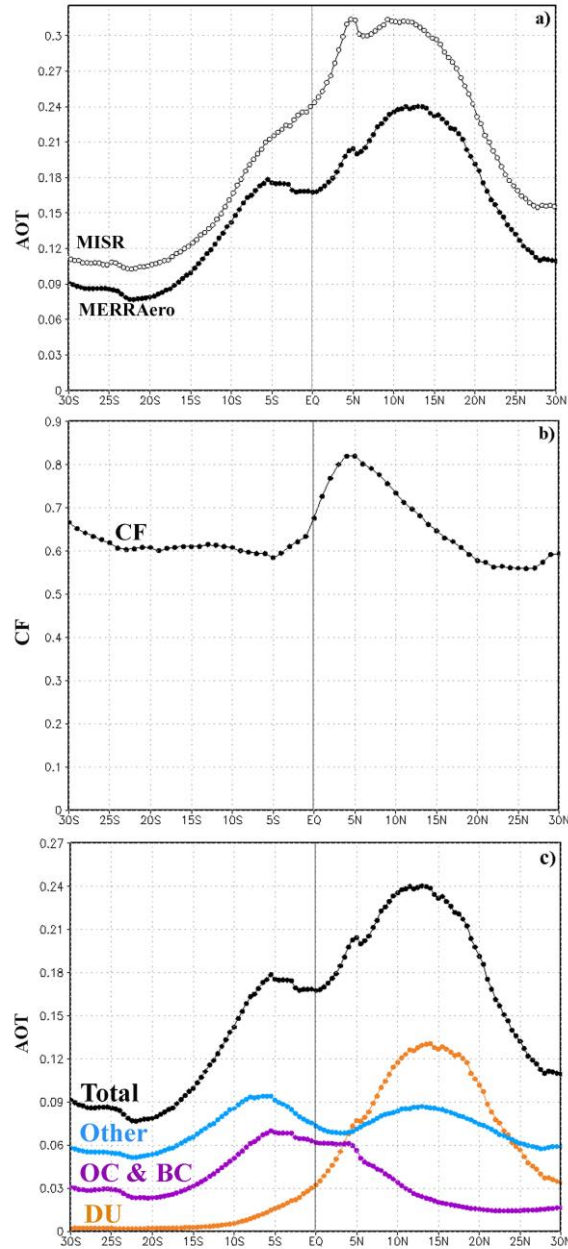
7



2 Figure 1. Spatial distributions of (a, c, and e) dust AOT (DU) and (b, d, and f) the ratio of DU  
 3 to AOT of all other aerosol species, based on the 10-y MERRAero data. In the right panel, the  
 4 red contour line represents the boundary of the zone where dust AOT is equal to AOT of all  
 5 other aerosol species.

6  
 7

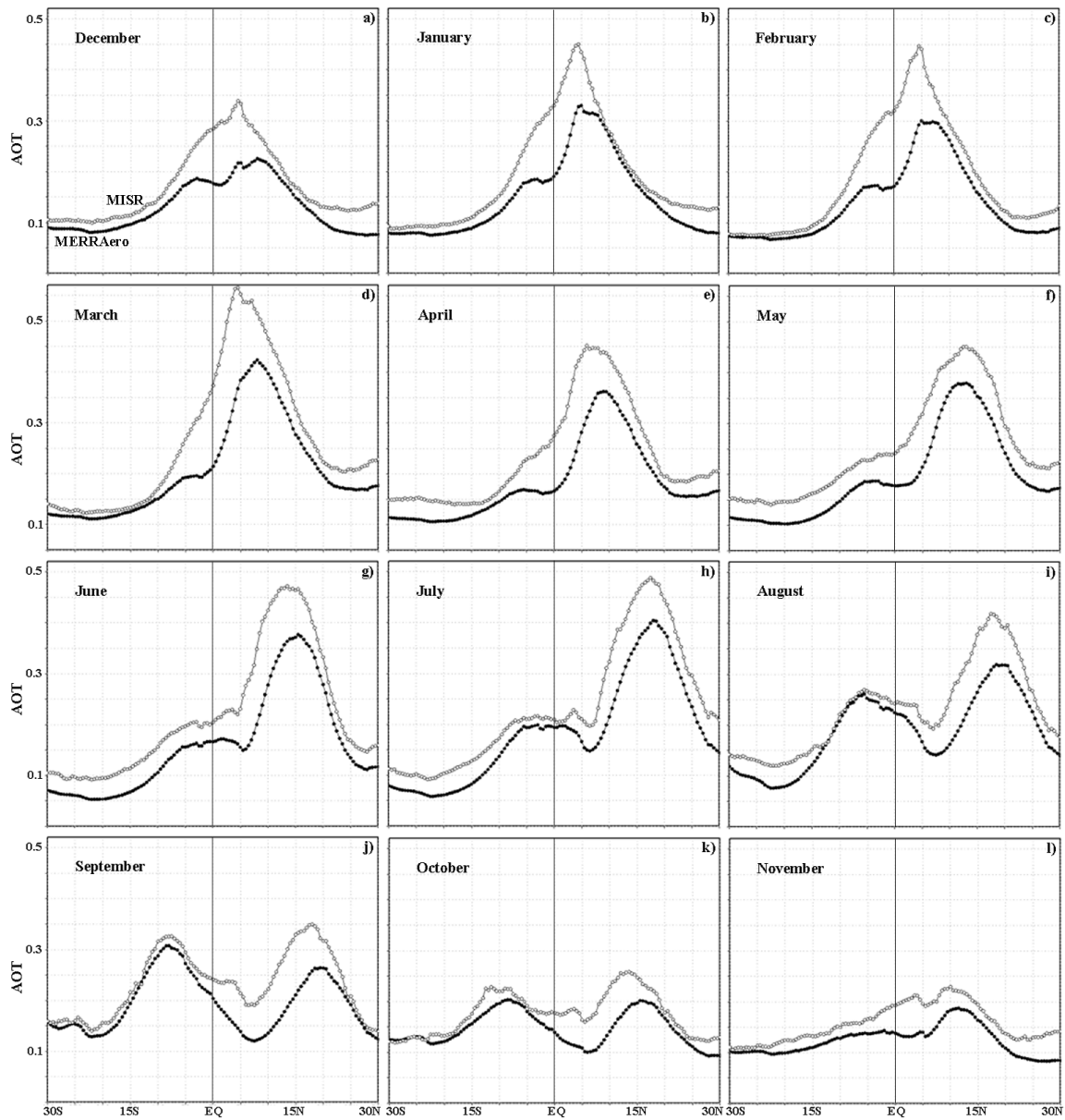
1



2

3 Figure 2. The meridional distribution of 10-year mean AOT/ CF, zonal averaged over the  
4 Atlantic Ocean ( $60^{\circ}\text{W} - 0^{\circ}\text{E}$ ): a –total AOT based on MERRAero and MISR data; b –  
5 MODIS CF, c - MERRAero total AOT, dust AOT (DU), organic and black carbon AOT (OC  
6 & BC), and other aerosol species AOT (Other). The vertical lines designate the position of the  
7 equator.

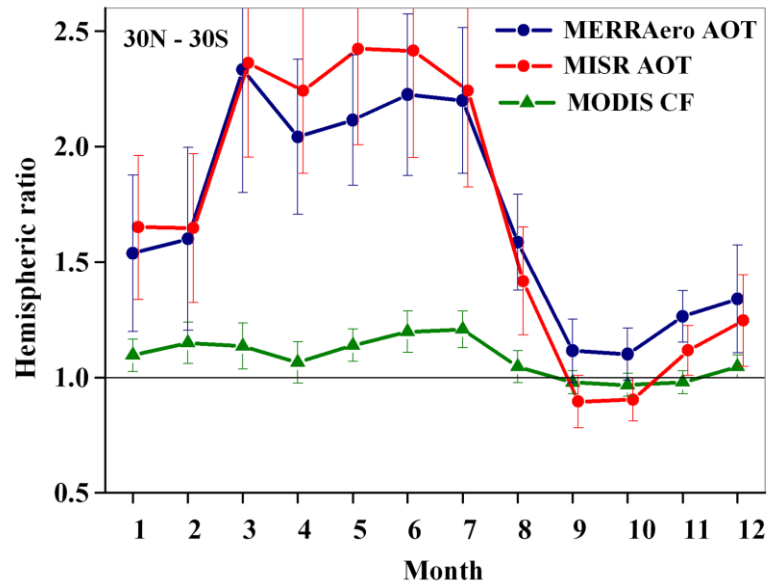
8



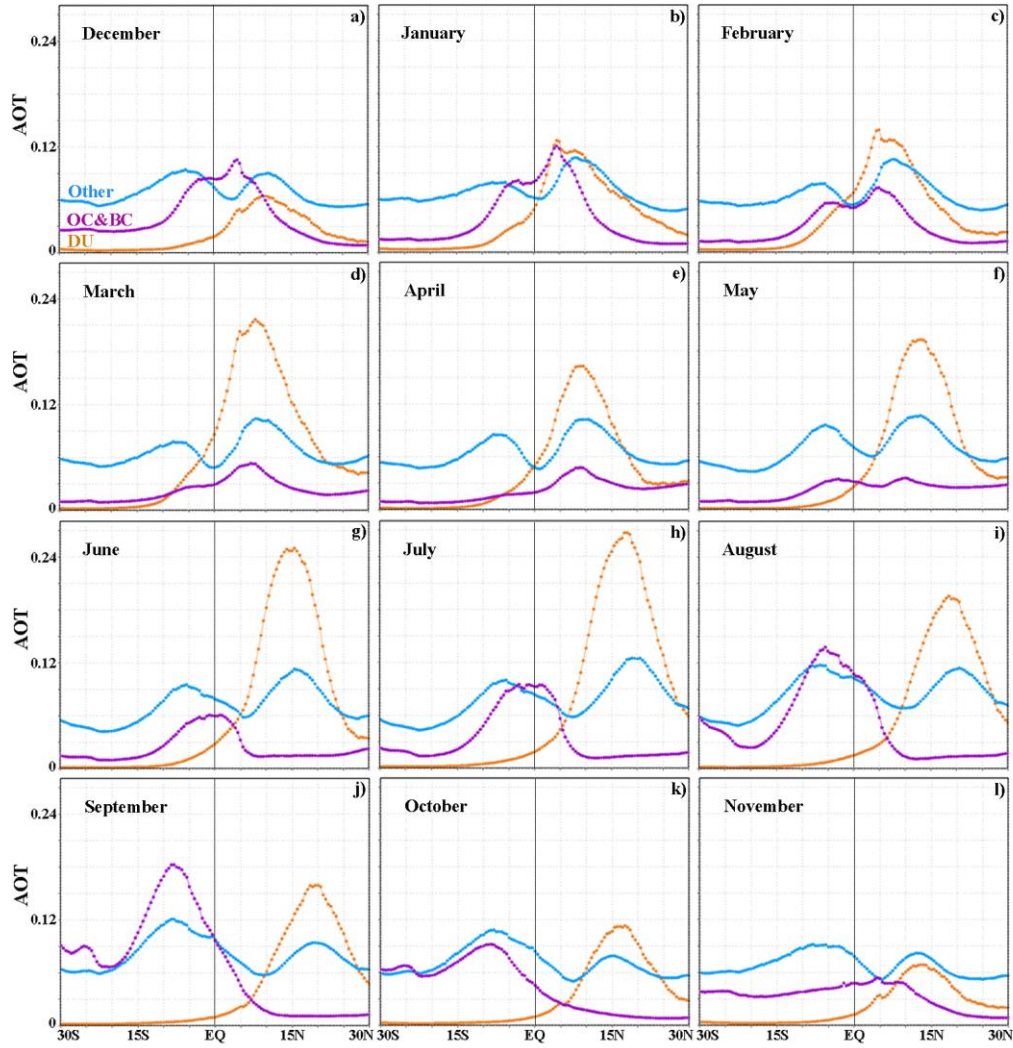
1  
 2 Figure 3. Meridional distribution of MISR and MERRAero total AOT, zonal averaged over  
 3 the Atlantic Ocean, for all months of the year. The vertical lines designate the position of the  
 4 equator.  
 5



1



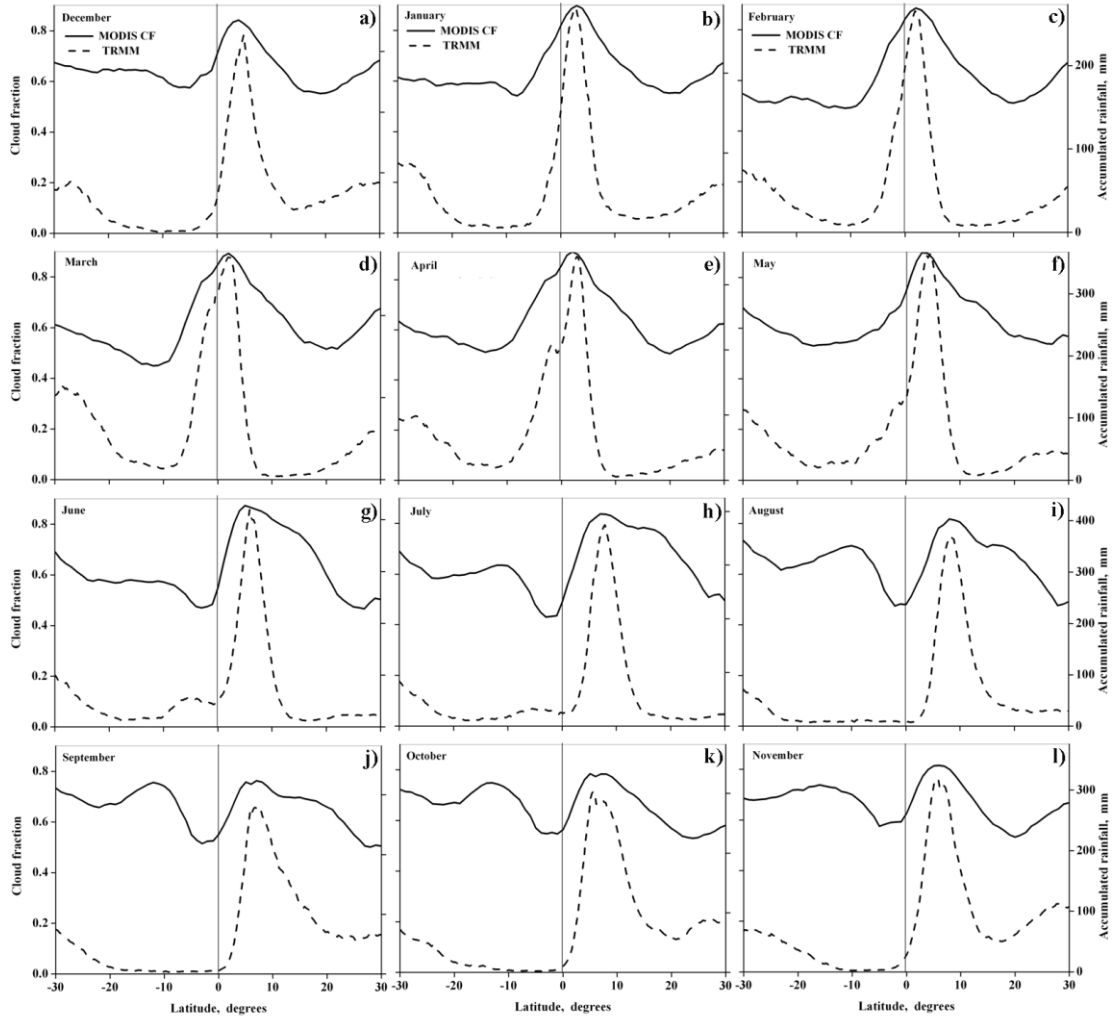
2 Figure 4. Month-to-month variations of the hemispheric ratio (R) of MISR AOT, MERRAero  
3 AOT and MODIS cloud fraction (CF) over the tropical Atlantic Ocean (30°N – 30°S). The  
4 error bars show the standard deviation of R.  
5



2  
3  
4  
5  
6  
7

Figure 5. Meridional distribution of dust AOT (DU), organic and black carbon aerosol AOT (OC & BC), and other aerosol species AOT (Other), zonal averaged over the Atlantic Ocean, for all months of the year, based on 10-year MERRAero data. The vertical lines designate the position of the equator.

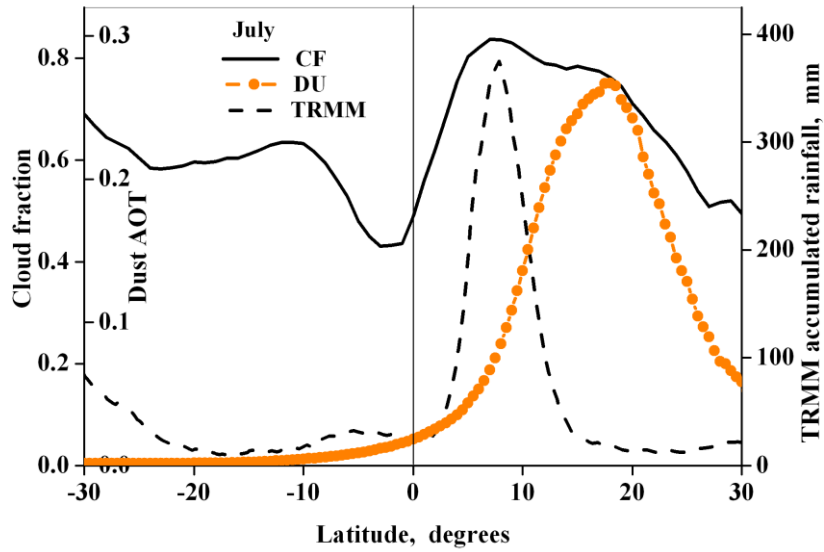
1



2  
3  
4  
5  
6

Figure 6. Meridional distribution of MODIS-Terra CF and TRMM accumulated rainfall, zonal averaged over the tropical Atlantic Ocean, for all months of the year. The vertical lines designate the position of the equator.

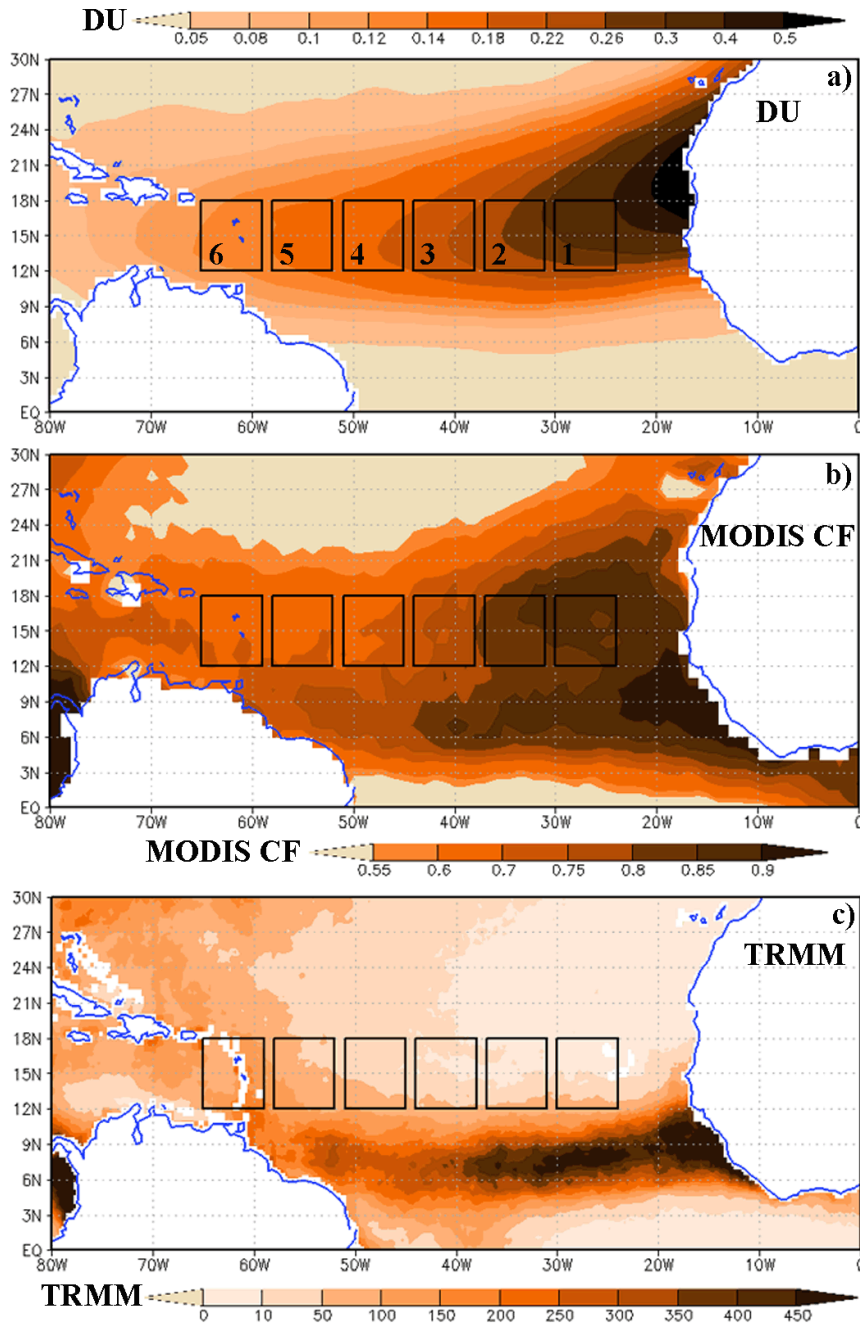
1



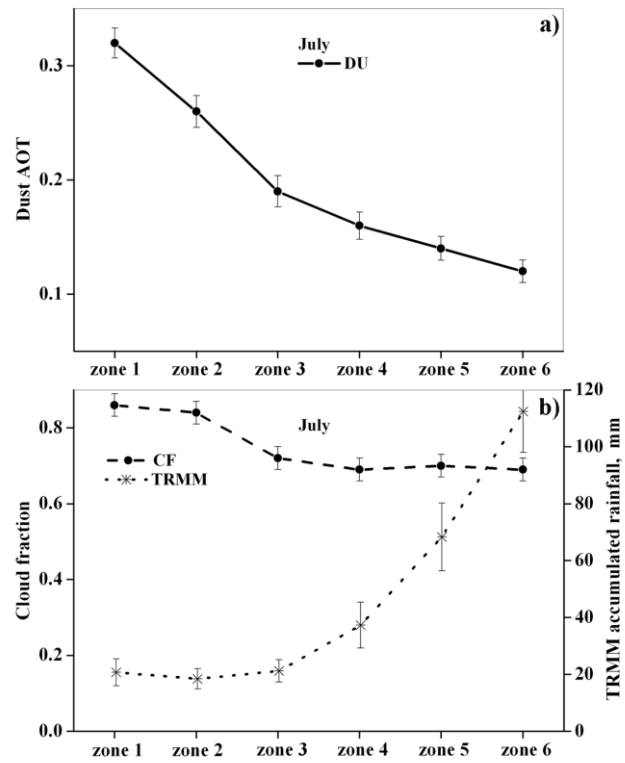
2

3 Figure 7. Meridional distribution of 10-year mean MODIS-Terra cloud fraction (CF), TRMM  
4 accumulated rainfall and MERRAero dust AOT (DU), zonal averaged over the Atlantic  
5 Ocean (60°W – 0°E), in July. The near-equatorial maximum in meridional distribution of  
6 TRMM accumulated rainfall indicates the position of the North Atlantic Ocean inter-tropical  
7 convergence zone (ITCZ). The vertical lines designate the position of the equator.

8



2 Figure 8. Spatial distributions of 10-year mean (a) MERRAero dust AOT (DU), (b) MODIS-  
 3 Terra CF, and (c) TRMM accumulated rainfall over the North Atlantic in July. The  
 4 geographic coordinates of the specified zones are as follows: zone 1 ( $12^{\circ}\text{N} - 18^{\circ}\text{N}$ ;  $30^{\circ}\text{W} -$   
 5  $24^{\circ}\text{W}$ ), zone 2 ( $12^{\circ}\text{N} - 18^{\circ}\text{N}$ ;  $37^{\circ}\text{W} - 31^{\circ}\text{W}$ ), zone 3 ( $12^{\circ}\text{N} - 18^{\circ}\text{N}$ ;  $44^{\circ}\text{W} - 38^{\circ}\text{W}$ ), zone 4  
 6 ( $12^{\circ}\text{N} - 18^{\circ}\text{N}$ ;  $51^{\circ}\text{W} - 45^{\circ}\text{W}$ ), zone 5 ( $12^{\circ}\text{N} - 18^{\circ}\text{N}$ ;  $58^{\circ}\text{W} - 52^{\circ}\text{W}$ ), zone 6 ( $12^{\circ}\text{N} - 18^{\circ}\text{N}$ ;  
 7  $65^{\circ}\text{W} - 59^{\circ}\text{W}$ ).

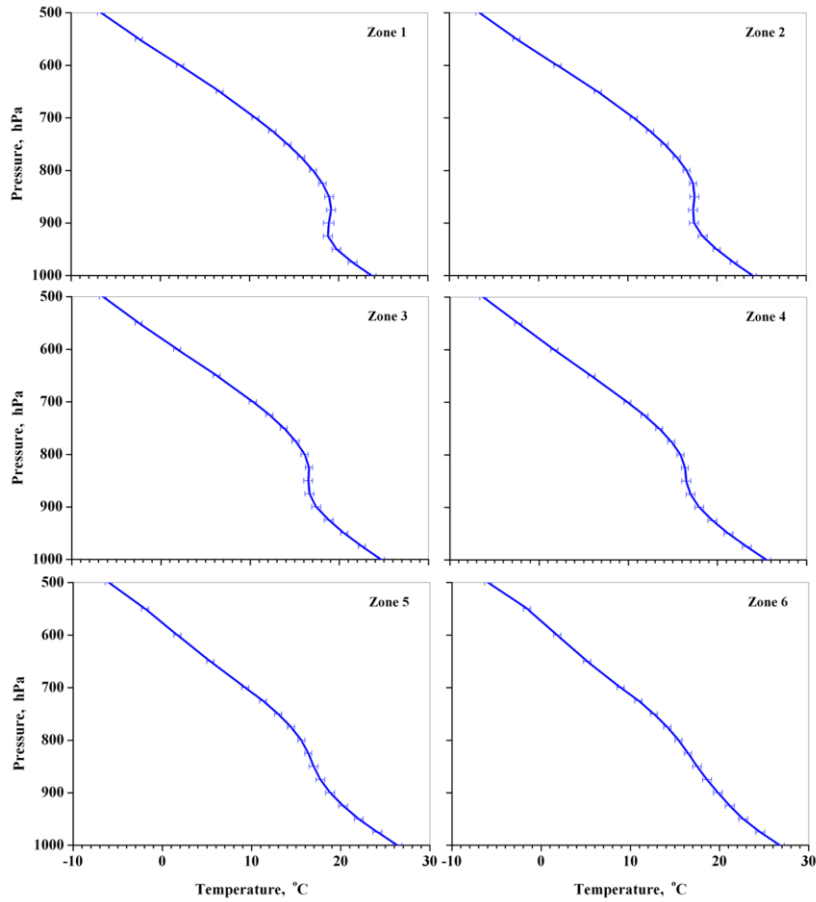


2

3 Figure 9. Zone-to-zone variations of (a) MERRAero dust AOT (DU); (b) MODIS-Terra CF  
 4 and TRMM accumulated rainfall over the specified zones in July, averaged over the ten-year  
 5 study period (2002 – 2012). The error bars show the standard error of mean.

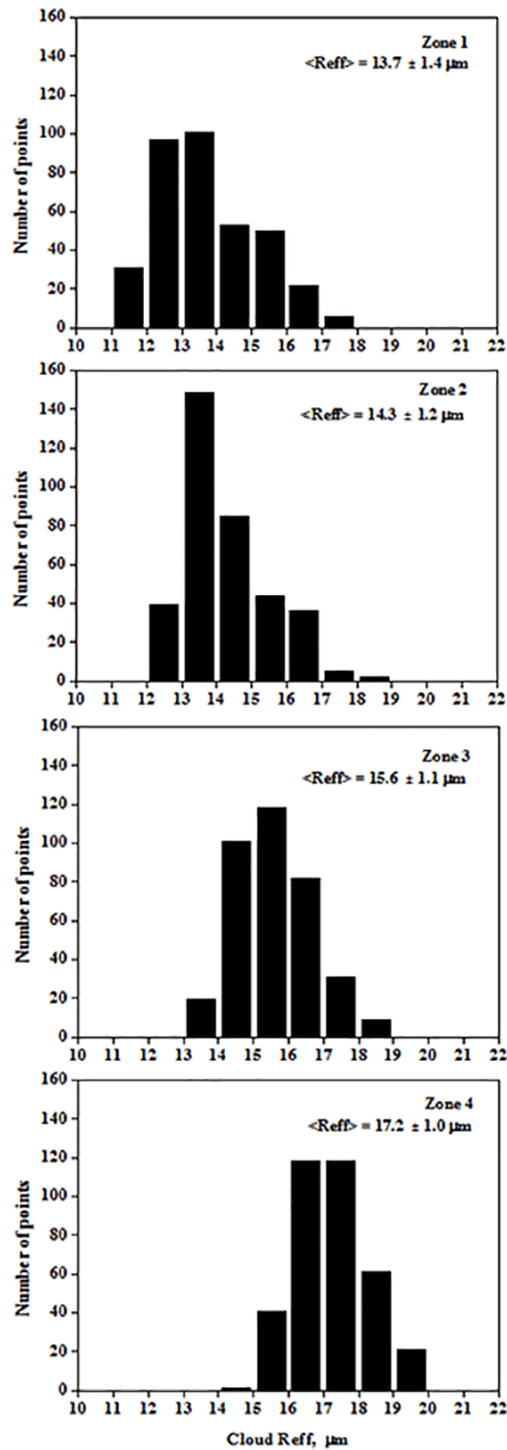
6

1



2 Figure 10. Vertical profiles of 10-year mean MERRA Reanalysis atmospheric temperature  
3 (°C) in July, averaged over the specified zones along the route of transatlantic dust transport.  
4 The error bars show the standard deviation of temperature.  
5

1  
2

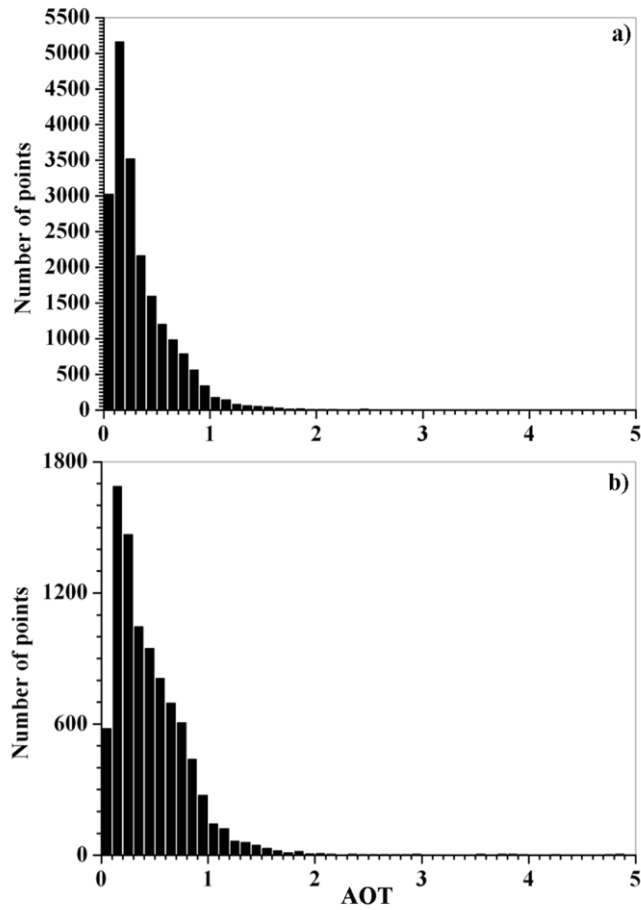


3  
4  
5  
6  
7  
8

Fig. 11. The histograms of effective particle radius ( $R_{eff}$ ) for liquid water clouds in the specified zones 1 – 4 along SAL, based on MODIS Level 3 gridded monthly data with resolution  $1^\circ \times 1^\circ$  during the 10-year study period in July. The average  $R_{eff}$  ( $\pm$  its standard deviation) in each zone is shown.



1  
2  
3



4  
5  
6  
7  
8  
9

Fig. 12. The histogram of AOT observed over the tropical North Atlantic in July 2010, based on Collection 5 MODIS-Terra Level 3 AOT daily data with resolution  $1^\circ \times 1^\circ$ : (a) over the tropical North Atlantic ( $30^\circ\text{N} - 0^\circ\text{N}$ ;  $60^\circ\text{W} - 0^\circ\text{E}$ ); (b) – over the latitudes with the SAL presence ( $12^\circ\text{N} - 24^\circ\text{N}$ ;  $60^\circ\text{W} - 0^\circ\text{E}$ ).